

**NASA  
Technical  
Paper  
2820**

1988

An Electrochemical Study  
of Corrosion Protection  
by Primer-Topcoat Systems  
on 4130 Steel With  
AC Impedance and DC Methods

M. J. Mendrek,  
R. H. Higgins,  
and M. D. Danford  
*George C. Marshall Space Flight Center  
Marshall Space Flight Center, Alabama*

**NASA**  
National Aeronautics  
and Space Administration

Scientific and Technical  
Information Division

## TABLE OF CONTENTS

	Page
INTRODUCTION.....	1
EQUIVALENT CIRCUITS.....	1
AC DATA ANALYSIS.....	5
EXPERIMENTAL.....	5
RESULTS AND DISCUSSION.....	11
Bare 4130 Steel.....	11
Zinc-Rich Primer Coated 4130 Steel.....	11
Red Lead Oxide Primer Coated 4130 Steel.....	17
Zinc-Rich Primer + 0.7 mils Topcoat.....	17
Red Lead Oxide Primer + 0.7 mils Topcoat.....	17
Zinc-Rich Primer + 2.3 mils Topcoat.....	30
Red Lead Oxide Primer + 2.6 mils Topcoat.....	41
Comparison of AC Impedance and DC Methods for Obtaining Corrosion Rates.....	41
CONCLUSIONS.....	49
REFERENCES.....	50

PRECEDING PAGE BLANK NOT FILMED

## LIST OF ILLUSTRATIONS

Figure	Title	Page
1.	Circuit representing AC impedance response for bare metals .....	2
2.	Circuit representing AC impedance response for primer coated and primer topcoated 4130 steel .....	2
3.	Physical description of circuit parameters for primer coated steel .....	3
4.	Alternate circuit representing AC impedance response for primer coated and primer top-coated 4130 steel .....	4
5.	Typical least-squares fit of Bode magnitude data – 0.6 mil zinc-rich primer, 0.7 mil topcoat .....	6
6.	Typical least-squares fit – 0.5 mil red lead oxide primer, 0.7 mil topcoat .....	7
7.	Typical least-squares fit – 1.6 mil zinc-rich primer, 2.3 mil topcoat .....	8
8.	Typical least-squares fit – 1.9 mil red lead oxide primer, 2.6 mil topcoat .....	9
9.	Exploded view of sample holder .....	10
10.	$E_{CORR}$ and $I_{CORR}$ versus time – zinc-rich primer .....	12
11.	$R_S$ , $C_S$ , and $C_f$ versus time – zinc-rich primer .....	13
12.	$R_f$ and $R_{total}$ versus time – zinc-rich primer .....	14
13.	$R_p$ and $C_c$ versus time – zinc-rich primer .....	15
14.	$R_t$ , $C_{dl}$ , and $C_{CR}$ versus time – zinc-rich primer .....	16
15.	$E_{CORR}$ and $I_{CORR}$ versus time - red lead oxide primer .....	18
16.	$R_S$ , $C_S$ , and $R_f$ versus time – red lead oxide primer .....	19
17.	$C_f$ , $R_p$ , and $C_c$ versus time – red lead oxide primer .....	20
18.	$R_t$ and $R_{total}$ versus time – red lead oxide primer .....	21
19.	$C_{dl}$ and $C_{CR}$ versus time – red lead oxide primer .....	22
20.	$E_{CORR}$ and $I_{CORR}$ versus time – zinc-rich primer + 0.7 mil topcoat .....	23

## LIST OF ILLUSTRATIONS (Concluded)

Figure	Title	Page
21.	$R_S$ and $C_S$ versus time – zinc-rich primer + 0.7 mil topcoat .....	24
22.	$R_f$ and $C_f$ versus time – zinc-rich primer + 0.7 mil topcoat .....	25
23.	$R_p$ and $C_c$ versus time – zinc-rich primer + 0.7 mil topcoat .....	26
24.	$C_{dl}$ and $C_{CR}$ versus time – zinc-rich primer + 0.7 mil topcoat .....	27
25.	$R_t$ and $R_{total}$ versus time – zinc-rich primer + 0.7 mil topcoat .....	28
26.	$E_{CORR}$ and $I_{CORR}$ versus time – red lead oxide primer + 0.7 mil topcoat .....	29
27.	$R_S$ and $C_S$ versus time – red lead oxide primer + 0.7 mil topcoat .....	31
28.	$R_f$ and $C_f$ versus time – red lead oxide primer + 0.7 mil topcoat .....	32
29.	$R_p$ and $C_c$ versus time – red lead oxide primer + 0.7 mil topcoat .....	33
30.	$R_t$ and $R_{total}$ versus time - red lead oxide primer + 0.7 mil topcoat .....	34
31.	$C_{dl}$ versus time – red lead oxide primer + 0.7 mil topcoat .....	35
32.	$E_{CORR}$ and $I_{CORR}$ versus time – zinc-rich primer + 2.3 mils topcoat .....	36
33.	$R_S$ , $C_S$ , and $C_f$ versus time – zinc-rich primer + 2.3 mils topcoat .....	37
34.	$R_f$ , $R_t$ , and $C_{dl}$ versus time – zinc-rich primer + 2.3 mils topcoat .....	38
35.	$(R_t + R_f)$ , $I_{CORR}$ (impedance), and $R_{total}$ versus time – zinc-rich primer + 2.3 mils topcoat .....	39
36.	$R_p$ , $C_c$ , and $C_{CR}$ versus time – zinc-rich primer + 2.3 mils topcoat .....	40
37.	$E_{CORR}$ and $I_{CORR}$ versus time – red lead oxide primer + 2.6 mils topcoat .....	42
38.	$R_S$ , $C_S$ , and $C_f$ versus time – red lead oxide primer + 2.6 mils topcoat .....	43
39.	$R_f$ , $R_t$ , and $C_{dl}$ versus time – red lead oxide primer + 2.6 mils topcoat .....	44
40.	$R_p$ , $C_c$ , and $C_{CR}$ versus time – red lead oxide primer + 2.6 mils topcoat .....	45
41.	$(R_t + R_f)$ , $I_{CORR}$ (impedance), and $R_{total}$ versus time – red lead oxide primer + 2.6 mils topcoat .....	46
42.	Calibration curve for $C_{CR}$ .....	48

**AN ELECTROCHEMICAL STUDY OF CORROSION PROTECTION BY  
PRIMER-TOPCOAT SYSTEMS ON 4130 STEEL  
WITH AC IMPEDANCE AND DC METHODS**

INTRODUCTION

As part of a general development of the AC impedance method in the study of corrosion of coated metals, this work, involving 4130 steel coated with primer-topcoat combinations, was undertaken. (For review of the AC impedance method, the reader is referred to three papers [1,2,3], which should prove beneficial in understanding the AC impedance technique.) No investigations by the AC impedance technique have previously been reported for metals coated with both primer and topcoat. Applicability of the present work to the Space Shuttle Transportation System lies in the relation to the coating system presently employed for the Solid Rocket Boosters (SRB). The 4130 steel basis metal was employed in this work because of its similarity to the D6AC steel forming the case of the SRB. Also, certain parts of the SRB are comprised of 4130 steel. One of the primer-topcoat systems studied, zinc-rich epoxy primer with epoxy-polyamide topcoat, is presently used for coating the SRBs. The other system, red lead oxide epoxy primer with epoxy-polyamide topcoat, was studied for comparison. As part of this work, the development of an equivalent circuit model suitable for describing the corrosion behavior of metal-primer-topcoat systems was necessary. In addition, ways for obtaining corrosion rates from AC impedance methods were investigated.

**EQUIVALENT CIRCUITS**

The basis of the AC impedance method is the modeling of the corrosion cell in terms of a purely electronic circuit. A suitable equivalent circuit should reasonably reproduce experimental plots obtained from the corrosion cell when experimentally determined parameters are used. These plots include Bode magnitude (impedance versus  $\log W$ , where  $W = 2\pi \times \text{frequency}$ ), Bode phase, and complex plane or Nyquist plot ( $-Z''$  versus  $Z'$ ). Previous investigations [1,2] have demonstrated that the equivalent circuit shown in Figure 1 best represents the AC impedance response of a corroding bare metal surface. Equivalent circuits for coated metal surfaces, however, are more complex, requiring additional resistor/capacitor combinations. The equivalent circuit in Figure 2 has been used successfully to represent the response of primer coated 2219-T87 aluminum [3]. The physical model this circuit represents is shown in Figure 3.

Research involving primer-topcoated steel corroding in seawater has not led to a single equivalent circuit that best fits the experimental data for the duration of the testing period. Rather, it was determined that while the equivalent circuit in Figure 2 works well for all systems, the equivalent circuit in Figure 4 usually produces a better fit when least squares convergence can be obtained. The difference between them is the addition of a capacitor to account for chemical reactions at the metal surface. Under some conditions the value of this capacitor is so large that its contribution to the impedance is nil. This, in

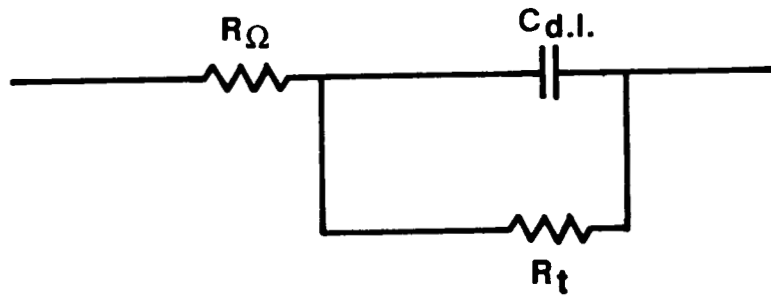
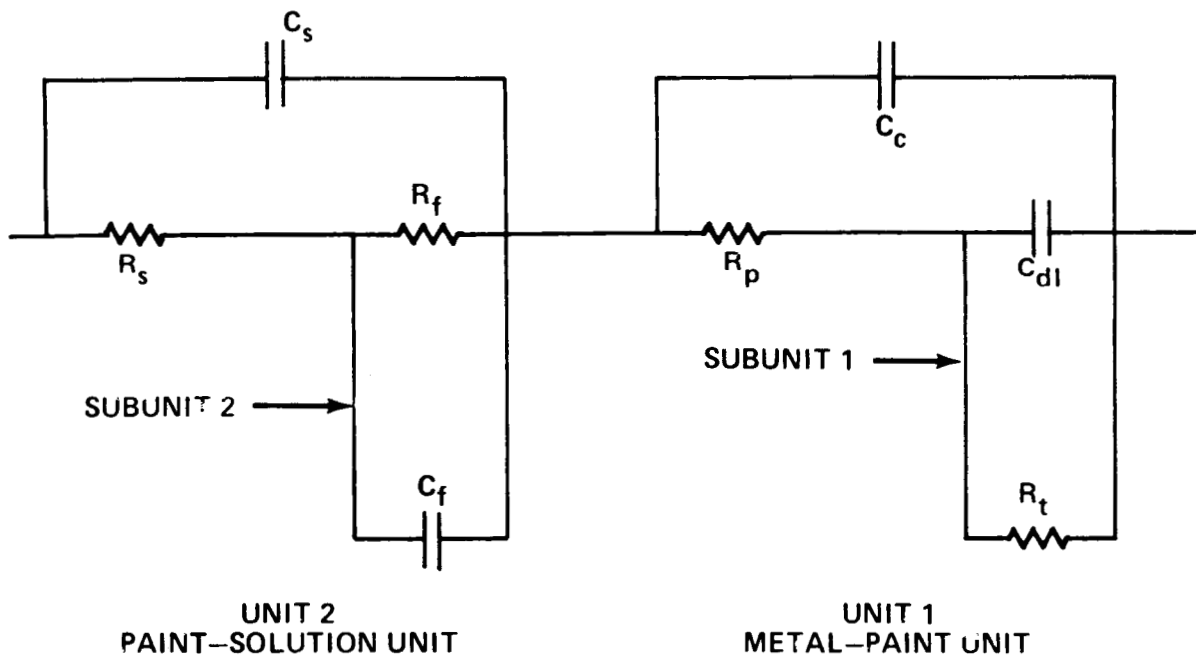


Figure 1. Circuit representing AC impedance response for bare metals.



$C_s$	SOLUTION CAPACITANCE
$R_s$	SOLUTION RESISTANCE
$C_f$	FARADAIC CAPACITANCE (COATING/SOLUTION)
$R_f$	FARADAIC RESISTANCE
$C_c$	COATING CAPACITANCE
$R_p$	COATING RESISTANCE
$C_{dl}$	METAL/COATING INTERFACE CAPACITANCE
$R_t$	CHARGE TRANSFER RESISTANCE

Figure 2. Circuit representing AC impedance response for primer coated and primer topcoated 4130 steel.

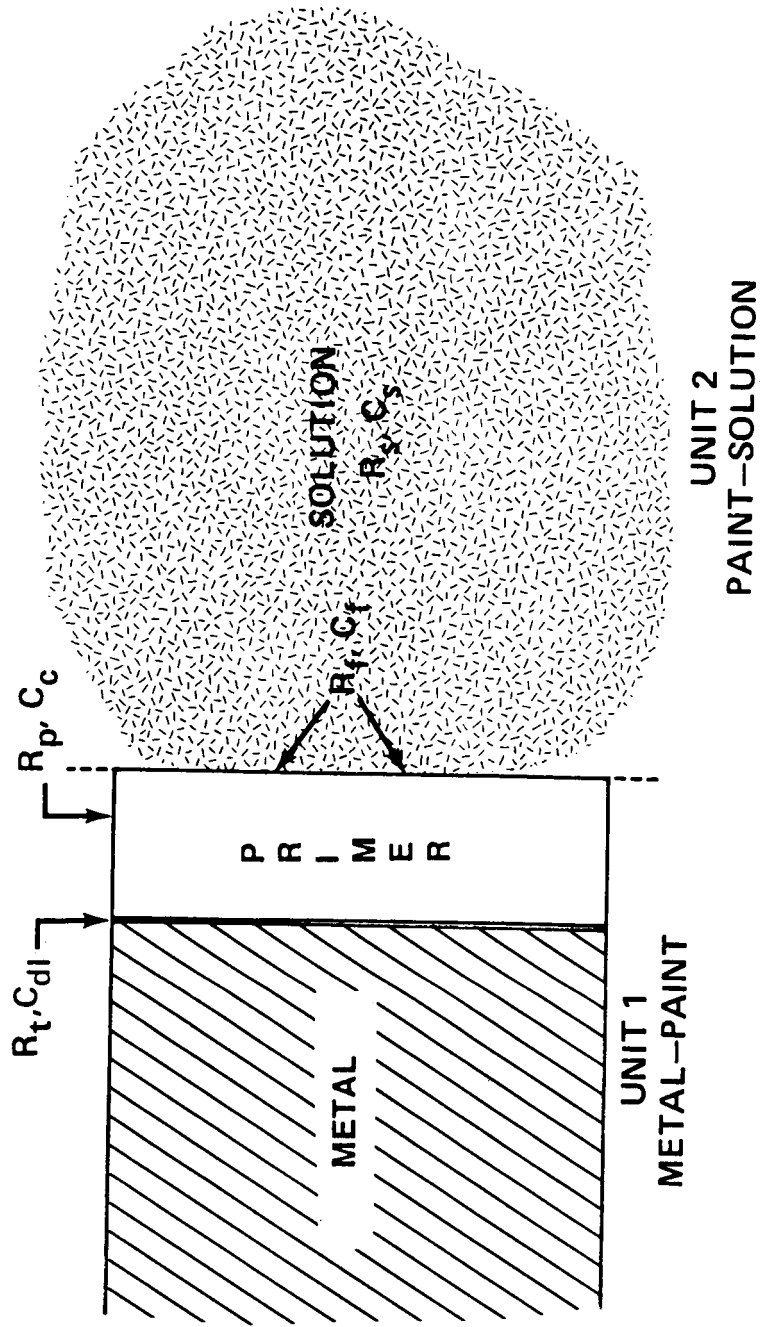
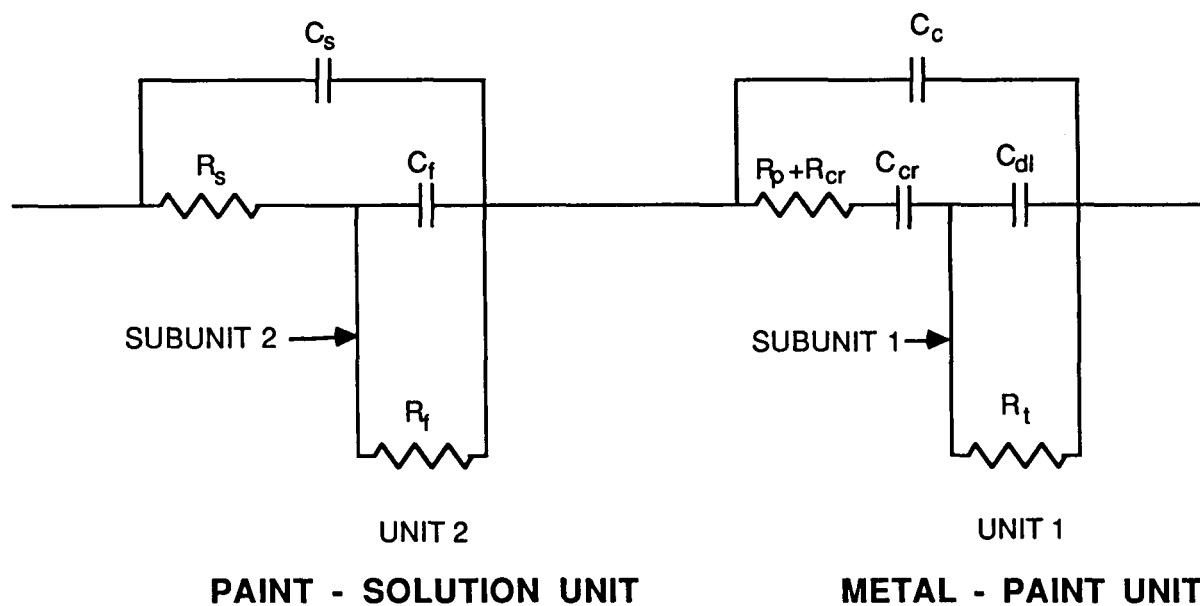


Figure 3. Physical description of circuit parameters for primer coated steel.

effect, short circuits the capacitor, making the circuit in Figure 4 the equivalent of that in Figure 2. In practice, it was found that the value of the additional capacitor ( $C_{CR}$ ) in Figure 4 is directly proportional to the corrosion current in cases where this capacitance can be determined in a least squares fitting procedure. Once this capacitor is "calibrated," the calibration curve, which is linear, can be used to obtain the corrosion current from AC impedance data for any system in which this model is applicable. Thus, the addition of this capacitor provides a useful way to obtain corrosion currents using the AC impedance method. Also, the models of Figures 2 and 4 can be used not only for metals coated with primer only, but also for metals coated with primer-topcoat systems. With such systems, the parameters for the primer and topcoat completely dominate, with those for the solution being completely overshadowed.



- $C_s$  SOLUTION CAPACITANCE
- $R_s$  SOLUTION RESISTANCE
- $C_f$  FARADAIC CAPACITANCE (COATING/SOLUTION)
- $R_f$  FARADAIC RESISTANCE
- $C_c$  COATING CAPACITANCE
- $R_p + R_{cr}$  COATING RESISTANCE + CHEMICAL REACTION RESISTANCE
- $C_{dl}$  METAL/COATING INTERFACE CAPACITANCE
- $R_t$  CHARGE TRANSFER RESISTANCE
- $C_{cr}$  CHEMICAL REACTION CAPACITANCE

Figure 4. Alternate circuit representing AC impedance response for primer coated and primer top-coated 4130 steel.

## AC DATA ANALYSIS

The goals of analyzing AC impedance data are threefold: (1) determine the equivalent circuit that most accurately describes the corrosion cell; (2) assign the best possible values to resistors and capacitors in the equivalent circuit for that particular experiment (for this program it was found that experiments should be run every two days for about six weeks or until the corrosion rate stabilizes or the coating visibly deteriorates); and (3) determine the best parameters in the equivalent circuit to describe the corrosion rate. As sample immersion continues, all of the model parameters change, some more than others.

Reference 3 outlines the method of obtaining starting parameters from experimental Nyquist plots. These values are read into a complex least-squares program, which is based on an adaptation of the general nonlinear least-squares program ORGLS [4]. It gives the best values for the parameters in the equivalent circuit. The quality of fit of the Bode magnitude data ( $\text{Log } |Z|$  versus  $\text{Log } \omega$ ) for the primer-topcoat systems tested is shown in Figures 5 to 8. All systems are described by the model in Figure 2, with completely different parameters being required to fit the data.

## EXPERIMENTAL

This investigation was divided into three phases. In Phase I, 4130 steel was coated with red lead oxide and zinc-rich primers alone to compare corrosion resistance and to evaluate the new equivalent circuit (Fig. 4). In Phase II, a thin epoxy-polyamide topcoat was added. The purpose of this was threefold: (1) to determine any limitations of the electrochemical methods due to coating thickness, (2) to compare the corrosion resistance of the two systems, and (3) to determine which equivalent circuit best describes the corroding system. In Phase III, nominal coating thicknesses were used, with the same goals as Phase II. The actual coating thicknesses and test durations are shown in Table 1.

TABLE 1. SUMMARY OF PRIMER AND TOPCOAT THICKNESSES AND TEST DURATIONS

	Zinc-Rich Systems		Red Lead Oxide Systems		Duration (days)
	Primer Thickness (mils)	Topcoat Thickness (mils)	Primer Thickness (mils)	Topcoat Thickness (mils)	
Phase I	0.8	-	0.6	-	38
Phase II	0.6	0.7	0.5	0.7	50
Phase III	1.6	2.3	1.9	2.6	60

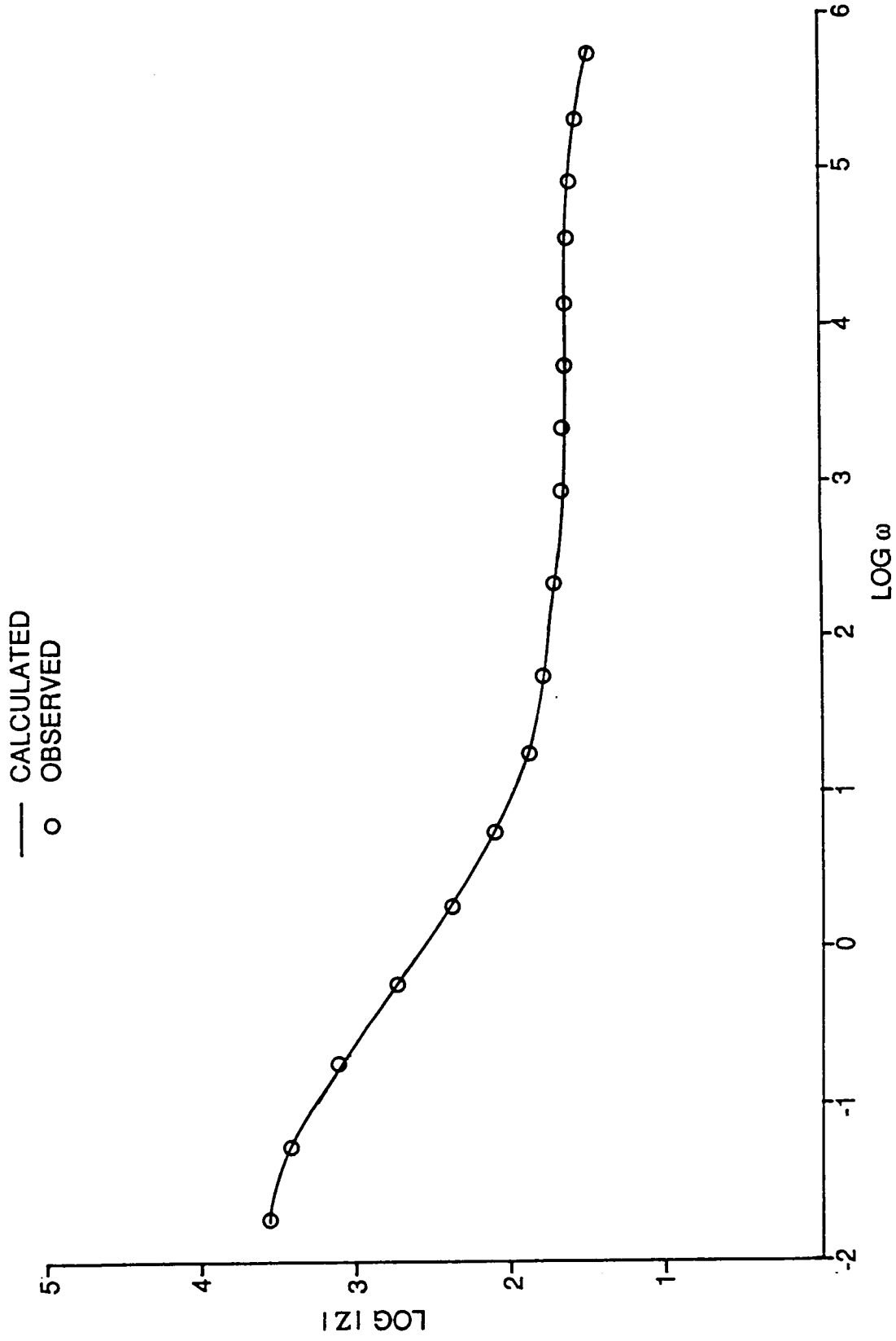


Figure 5. Typical least-squares fit of Bode magnitude data - 0.6 mil zinc-rich primer, 0.7 mil topcoat.

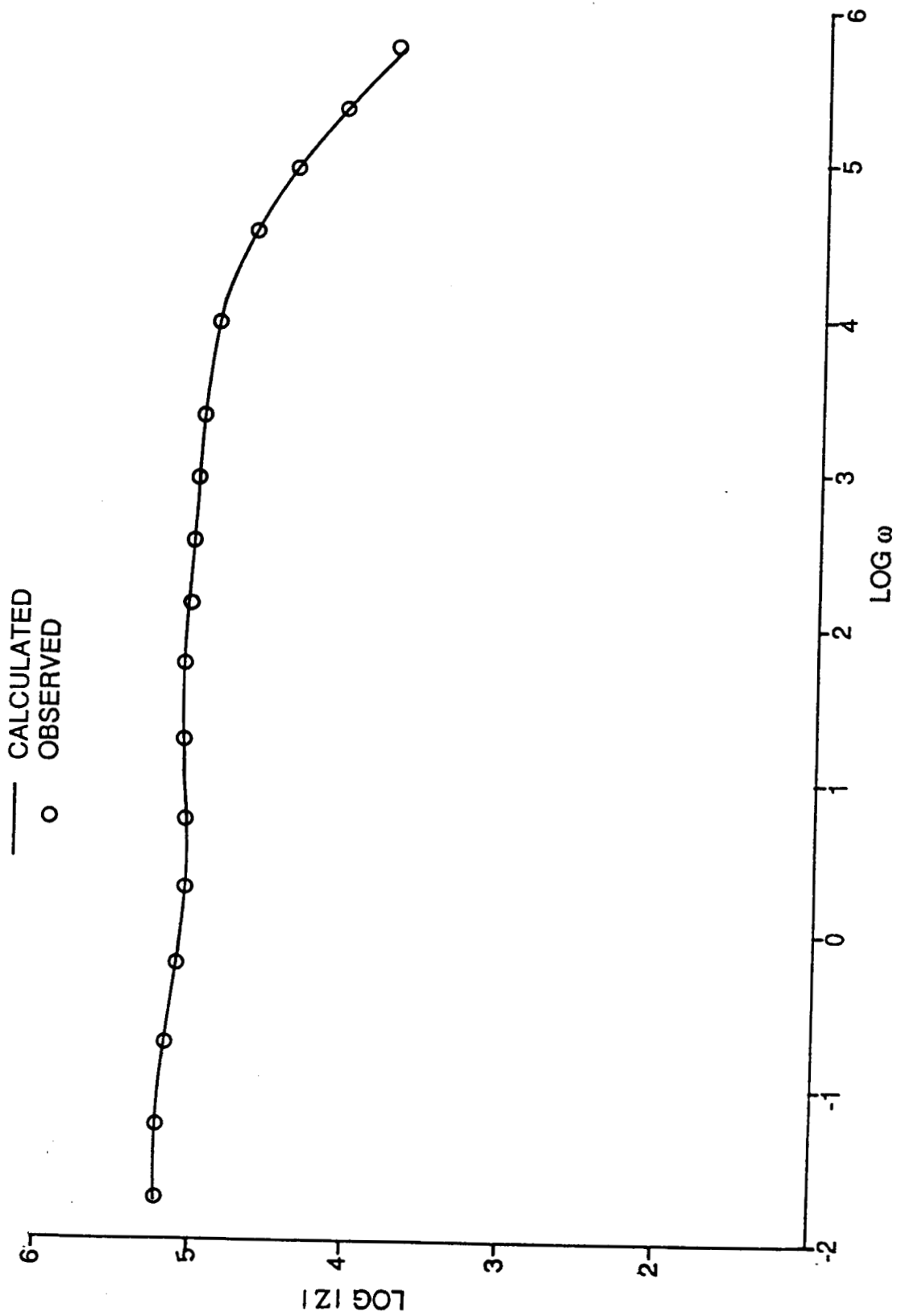


Figure 6. Typical least-squares fit - 0.5 mil red lead oxide primer, 0.7 mil topcoat.

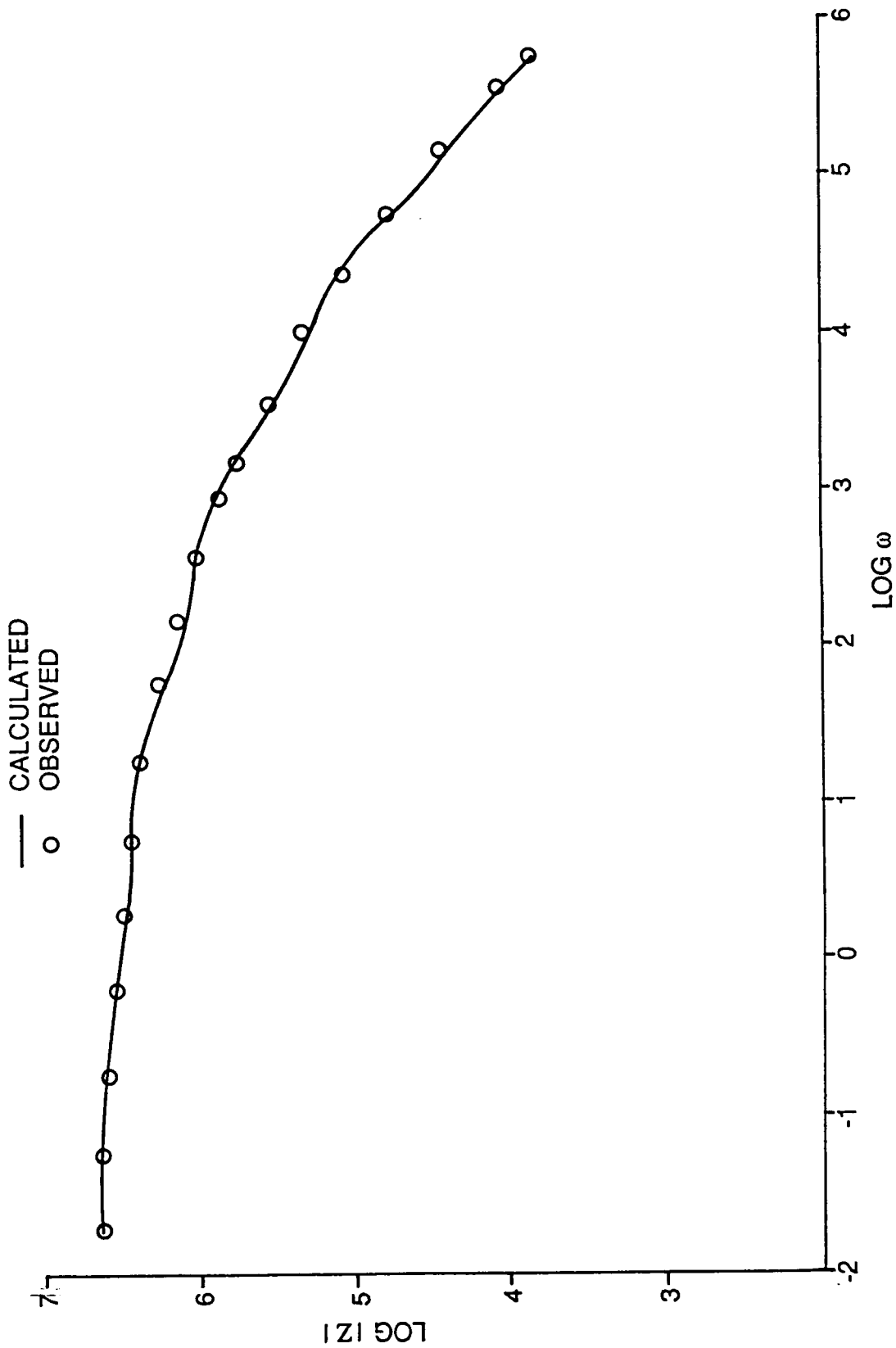


Figure 7. Typical least-squares fit - 1.6 mil zinc-rich primer, 2.3 mil topcoat.

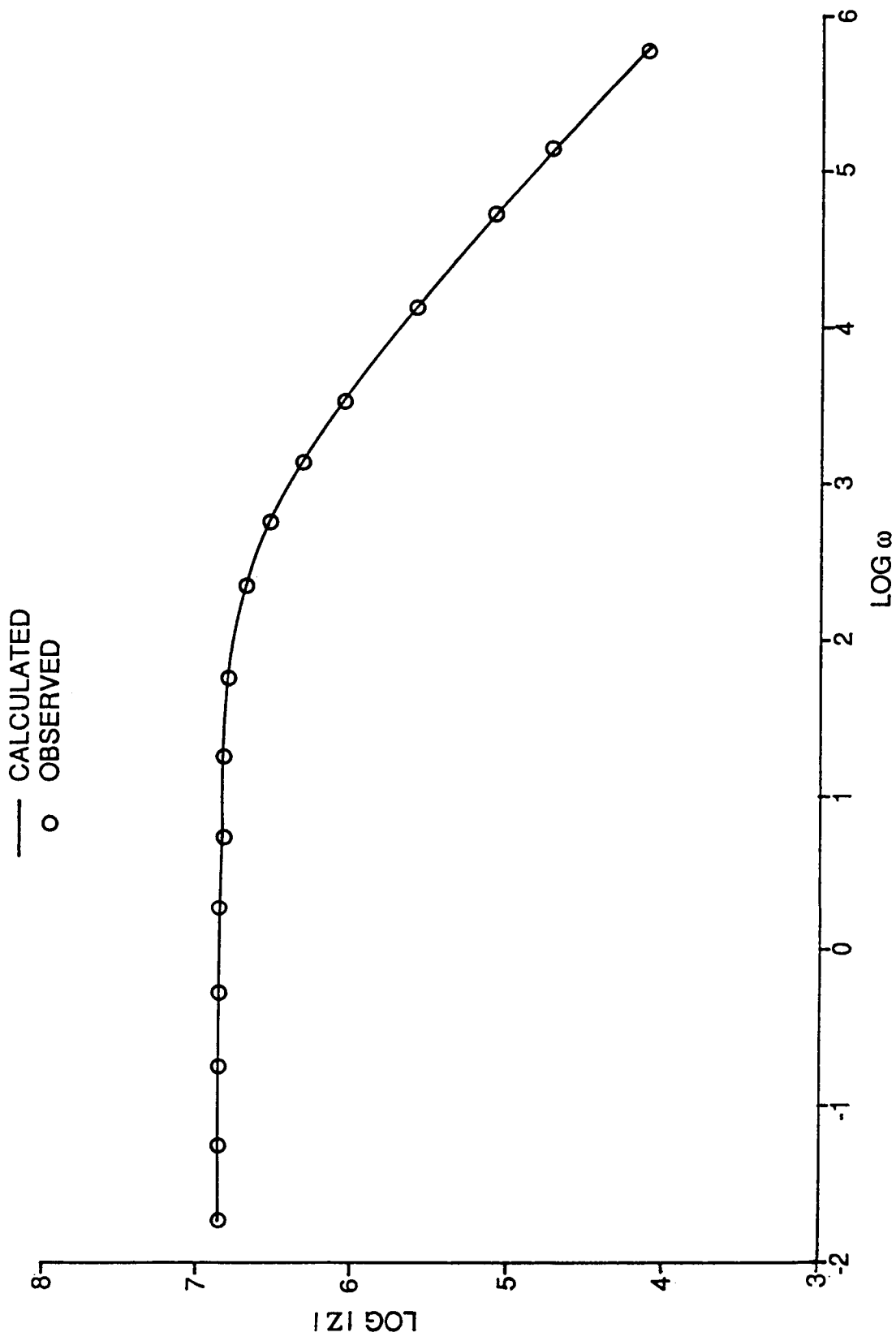


Figure 8. Typical least-squares fit - 1.9 mil red lead oxide primer, 2.6 mil topcoat.

AC impedance and polarization resistance (DC) measurements were made on alternating days for each phase of the test period. The 4130 specimens, which were 1.43 cm in diameter and 0.14 cm thick, were sand blasted, coated with the appropriate primer or primer-topcoat combination, cured to manufacturers' specifications, and immersed in a 3.5 percent NaCl solution buffered at pH 5.4 for the entire period. The sample holder, which exposes a sample with an area of 1.0 cm<sup>2</sup> to the test solution, is shown in Figure 9.

The EG&G-PARC Model 368 AC impedance system was used for both AC impedance and polarization resistance data collection. During each phase, data were taken on alternate days. AC impedance data were taken in three sections. The first two sections, beginning at 0.001 Hz and 0.1 Hz respectively, were obtained using the Fast Fourier Transform Technique (FFT). The last section, ranging from 5.7 Hz to 90,000 Hz, was collected using the lock-in amplifier technique. The sequencing was performed automatically using the auto-execute procedure, with all data being merged to a single set for each run. The period of collection of the AC impedance data was about 2.5 hr. After collection, the data were processed and analyzed as described in Reference 3 using the equivalent circuit models of Figures 2 and 4.

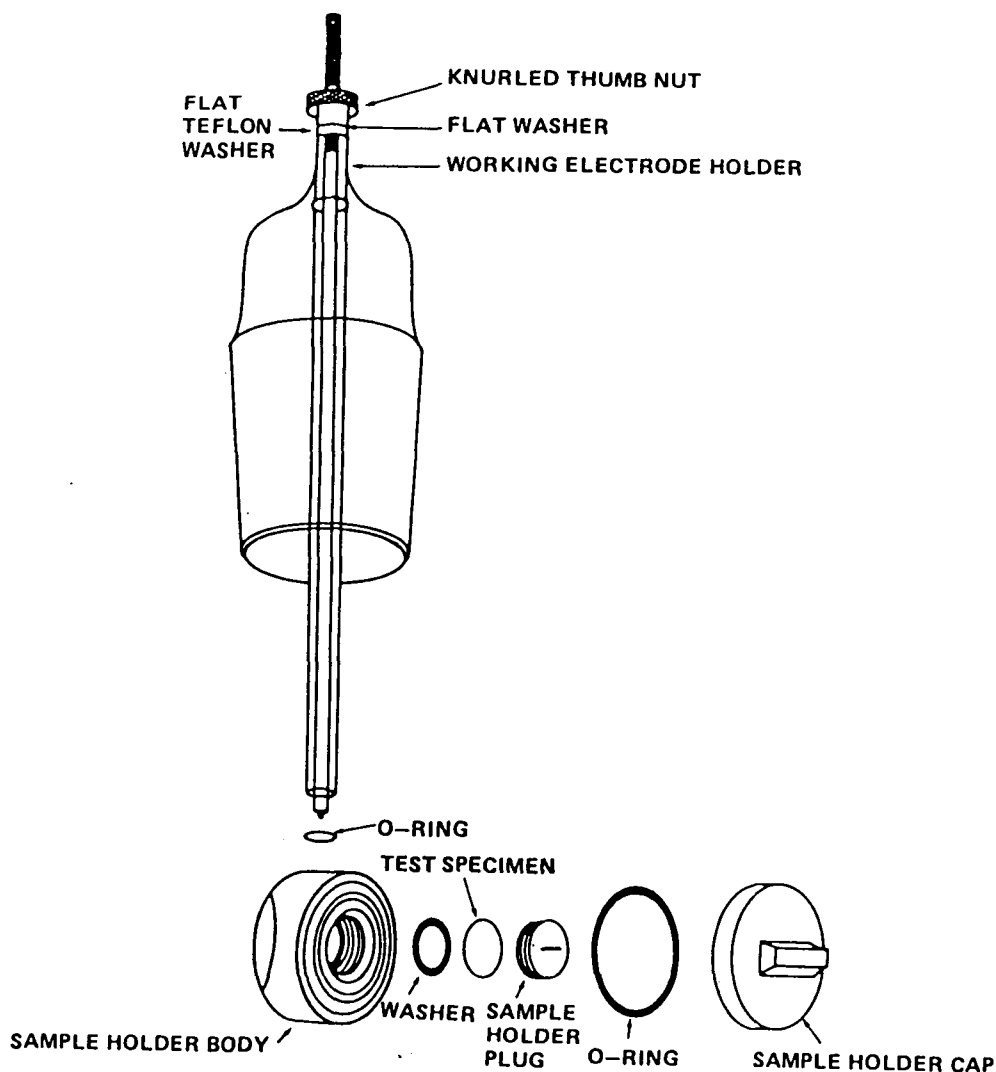


Figure 9. Exploded view of sample holder.

Data were collected for the polarization resistance method using the same system with the EG&G-PARC Model 332 Corrosion Measurement Software, which was developed especially for DC measurements. The data were automatically corrected during the scan for IR drop using the technique developed by EG&G-PARC. The data were transferred to a larger, faster computer and analyzed using the program POLCURR [5]. The theory for the polarization resistance technique has been described previously [6].

In addition to the foregoing, a sample of bare 4130 steel was studied at pH 5.4 in 3.5 percent NaCl using both the polarization resistance and AC impedance methods. A single run for each method was made, the AC impedance data being analyzed according to the model shown in Figure 1.

## RESULTS AND DISCUSSION

### Bare 4130 Steel

AC impedance data were obtained at pH 5.4 using the model shown in Figure 1. Values of 100 ohms, 1131 ohms, and 209  $\mu\text{F}$  were obtained for  $R_S$ ,  $R_t$ , and  $C_{dl}$ , respectively. The corrosion current, measured using the DC polarization resistance method, was 26.4  $\mu\text{A}/\text{cm}^2$ . The value of the polarization resistance obtained from this method was 1045 ohms. Thus, for 4130 steel, the value of  $R_t$  obtained with the AC impedance method is about the same as the polarization resistance obtained using the DC method. This is illustrated by passing direct current through the circuit in Figure 1. At zero frequency (the DC case) only resistive components contribute. These resistances are  $R_t$  and  $R_S$  with  $R_t$  being nearly equal to the polarization resistance obtained from the polarization resistance technique. Thus, the two methods are in very good agreement, which is very gratifying.

### Zinc-Rich Primer Coated Steel

The polarization resistance data ( $E_{\text{CORR}}$  and  $I_{\text{CORR}}$  versus time) are shown in Figure 10. As seen from the  $I_{\text{CORR}}$  versus time curve, the corrosion current is relatively large initially – possible due to a high initial dissolution rate of the zinc in the primer – but then drops off at about 4 to 5 days. Good protection is provided through day 24, after which the corrosion current rises steadily.

AC impedance data were analyzed using both models (Figs. 2 and 4), resulting in nine time-dependent plots (Figs. 11 to 14). In addition, the four resistance parameters were added together to produce a plot of the total resistance versus time (Fig. 12b). As expected, the capacitance generally increases and the resistance generally decreases with time; both conditions resulting in decreasing impedance. A few features, however, merit special attention. From Figure 12, it is obvious that  $R_F$  controls  $R_{\text{total}}$ , indicating that the corrosion rate is charge-transfer controlled. This is confirmed by extrapolation of the linear portion of the Bode magnitude plot to zero frequency. The sudden drop in resistances ( $R_f$ ,  $R_p$ , and  $R_t$ ) at about 10 days indicates the initiation of coating breakdown, as seen by a steady increase in  $I_{\text{CORR}}$  after 10 days. Further coating breakdown occurs at approximately 24 days, as illustrated in Figure 13b by a drastic increase in  $C_c$  and subsequent accelerated increase in  $I_{\text{CORR}}$ . Of particular interest is the similarity between the  $I_{\text{CORR}}$  and  $C_{\text{CR}}$  curves.

### ZINC RICH PRIMER

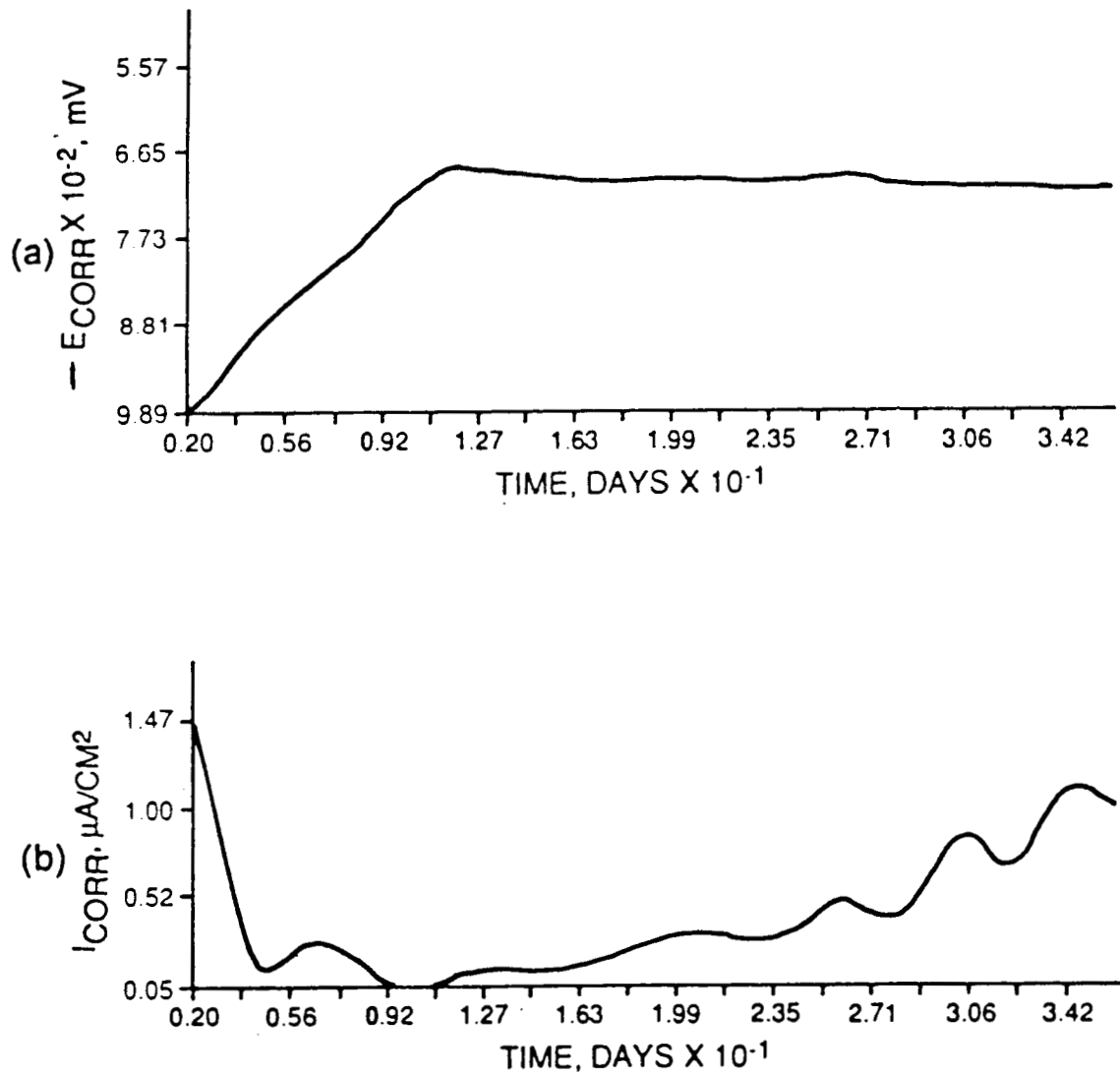


Figure 10.  $E_{CORR}$  and  $I_{CORR}$  versus time – zinc-rich primer.

### ZINC RICH PRIMER

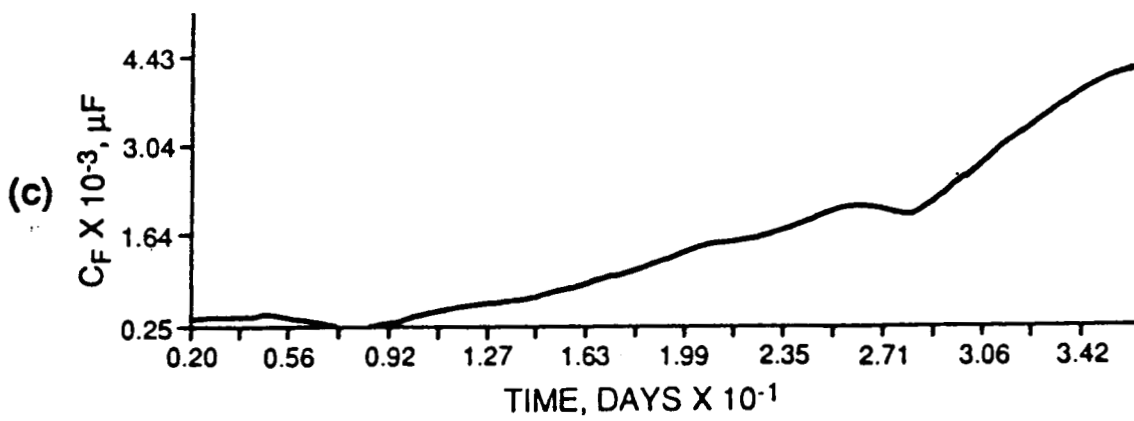
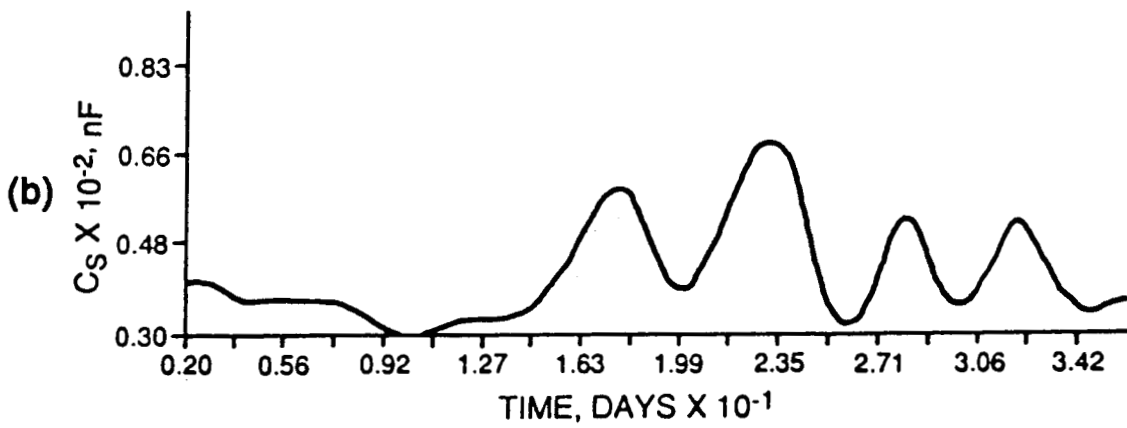
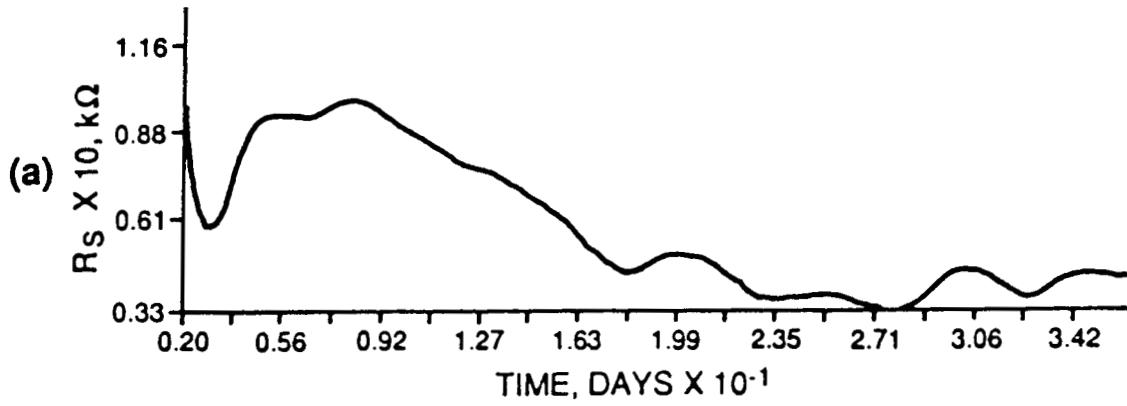


Figure 11.  $R_S$ ,  $C_S$ , and  $C_F$  versus time – zinc-rich primer.

### ZINC RICH PRIMER

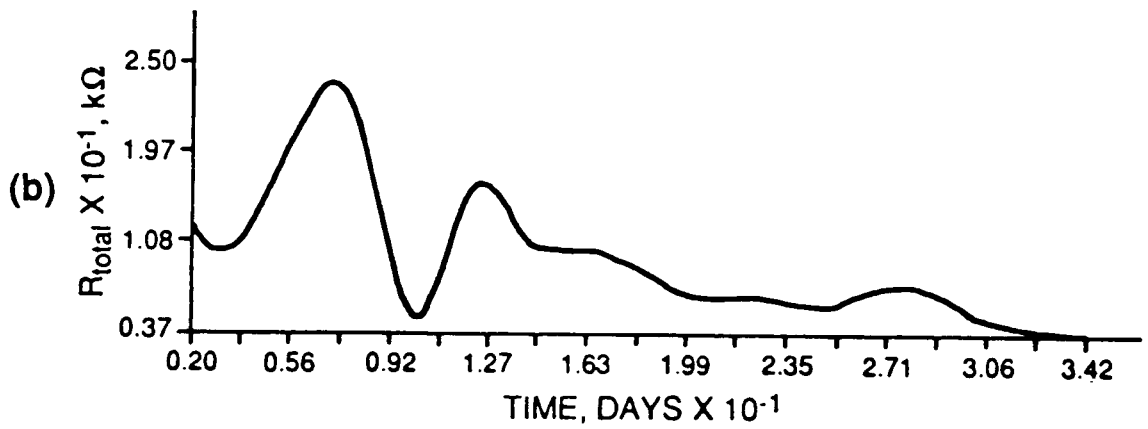
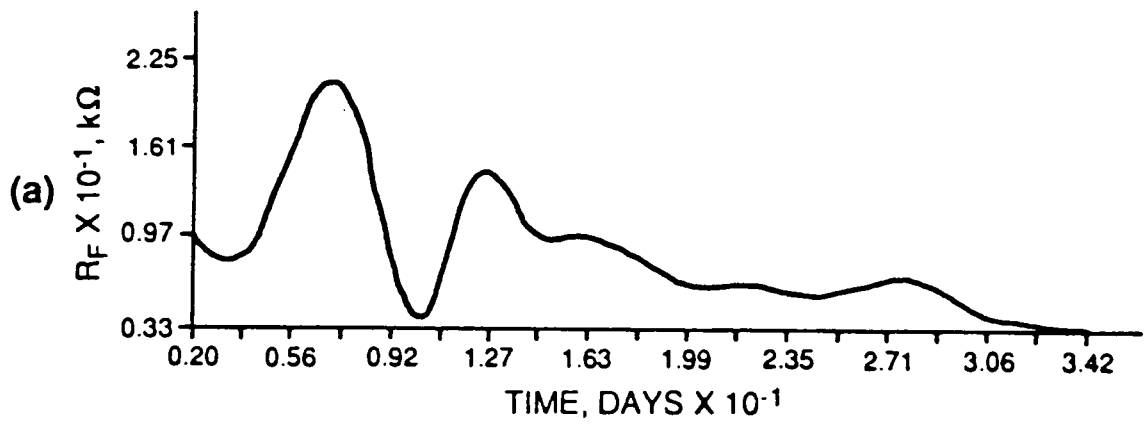


Figure 12.  $R_f$  and  $R_{total}$  versus time – zinc-rich primer.

### ZINC RICH PRIMER

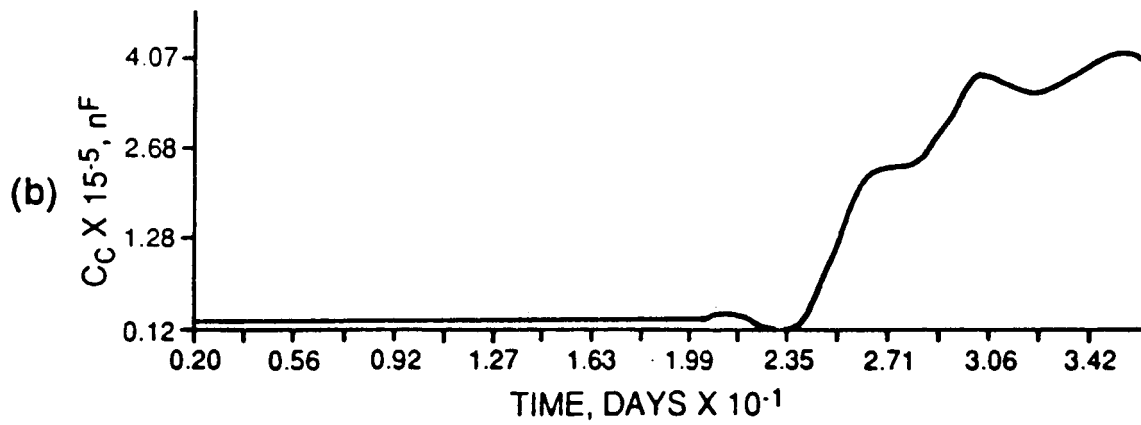
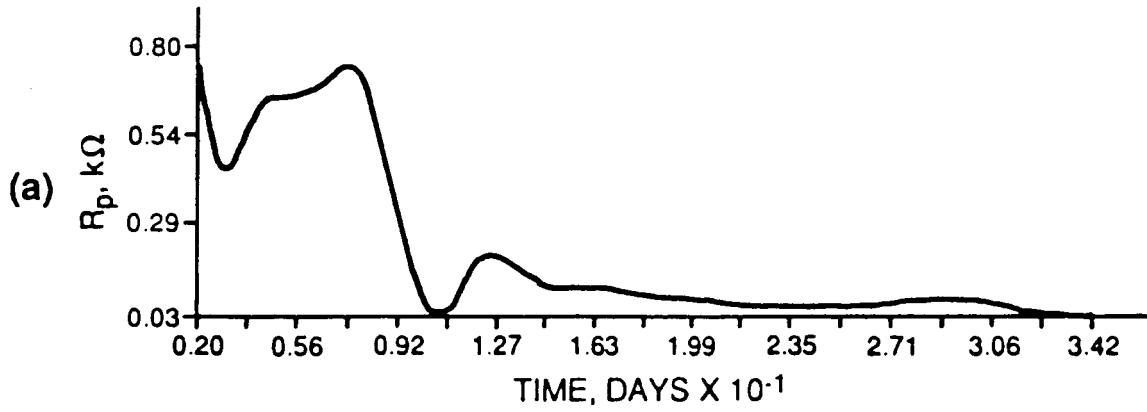


Figure 13.  $R_p$  and  $C_c$  versus time – zinc-rich primer.

### ZINC RICH PRIMER

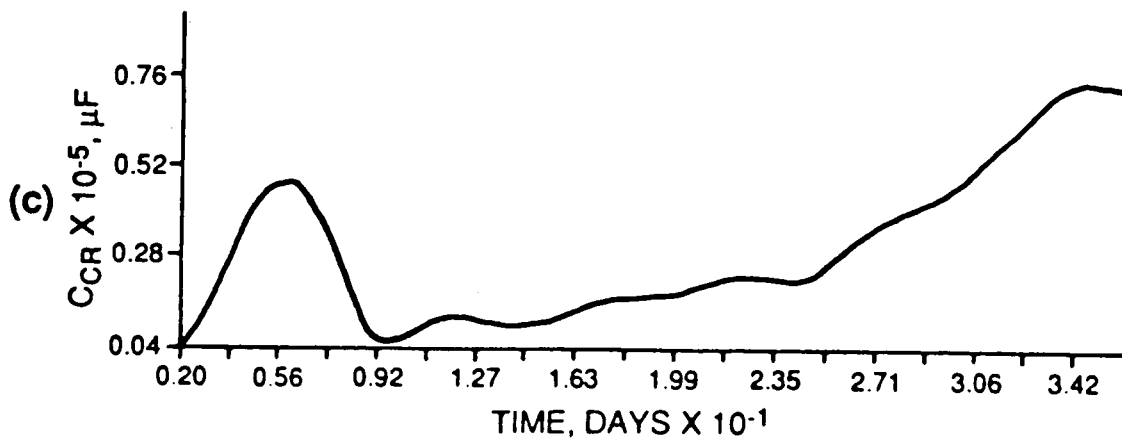
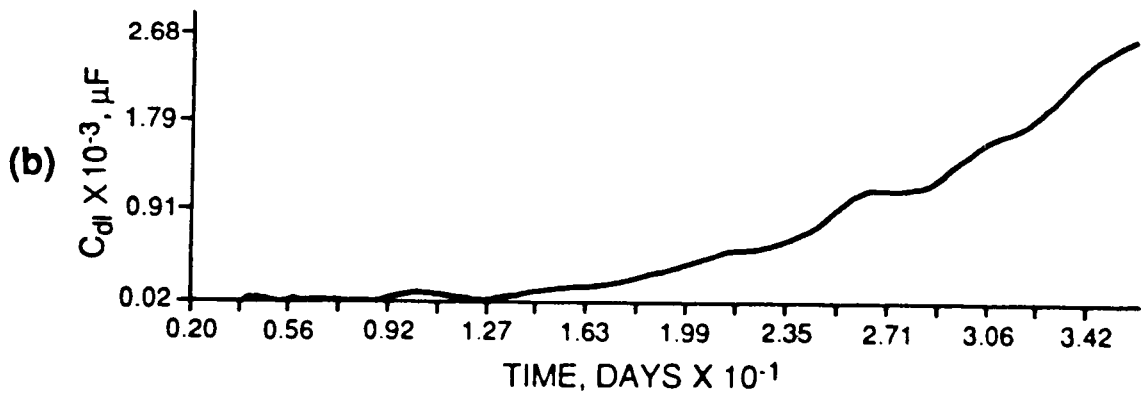
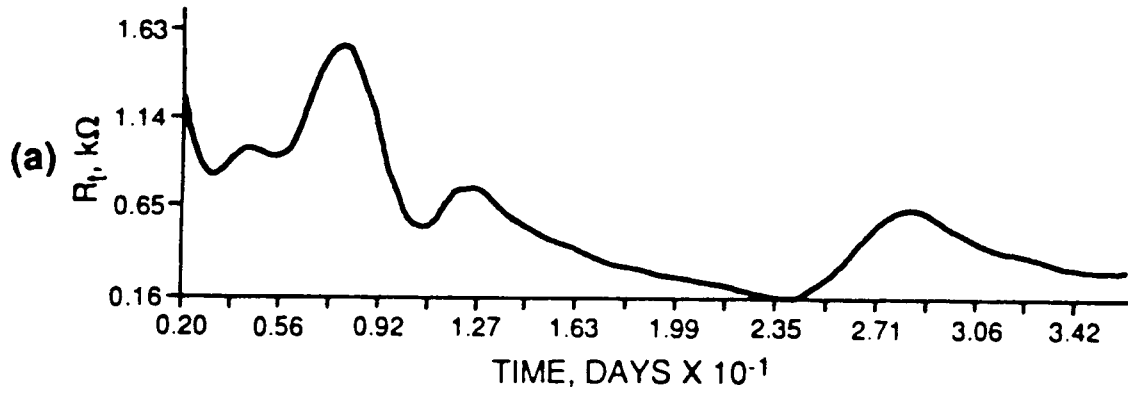


Figure 14.  $R_t$ ,  $C_{dl}$ , and  $C_{CR}$  versus time – zinc-rich primer.

## Red Lead Oxide Primer Coated Steel

The polarization resistance data for the red lead oxide primer coated steel are shown in Figure 15. The corrosion current rises steadily with time, reaches a maximum at about 16 days, then stabilizes at about 22 days. Comparing Figure 15b with Figure 10b illustrates the superior protection provided by the zinc-rich primer. AC impedance data are shown in Figures 16 to 19. Again, capacitance generally increases, while resistance decreases. However, in this case,  $R_t$  controls  $R_{total}$  (Fig. 18).

The small decrease in  $I_{CORR}$  at about 13 days is related to the maxima in the resistances  $R_t$  and  $R_p$ . More importantly, the peak in  $I_{CORR}$  at 17 days corresponds to a decrease in all resistances, and to an increase in  $C_{CR}$  and  $C_f$ . (AC impedance measurements are more sensitive to changes in the nature of the sample, thus leading DC responses by about a day.) All of these factors result in decreased impedance, and therefore increased corrosion current. Again, the  $C_{CR}$  versus time curve bears resemblance to the  $I_{CORR}$  versus time curve. It is worth noting that  $C_c$  (Fig. 17c) does not increase with time as do the other capacitors in the circuit.

## Zinc-Rich Primer with 0.7 Mils Topcoat

The  $E_{CORR}$  and  $I_{CORR}$  time curves are shown in Figure 20. Breakdown of the paint system appears to begin at around 28 days, as illustrated by an increase in the corrosion current. This is supported by the detection of tiny blisters on the topcoat, which were first observed on the 28th day. On comparing the  $I_{CORR}$  versus time curves for the zinc-rich primer alone and the zinc-rich primer with topcoat, there is no apparent increase in corrosion protection provided by the 0.7 mils of topcoat after 28 days.

AC impedance data are shown in Figures 21 to 25. As expected, values of resistors and capacitors follow trends toward decreasing impedance. The value of  $R_s$  (Fig. 21), however, is much larger and represents a larger portion of the total resistance than in the case of primer alone. This leads to the conclusion that  $R_s$  represents not only the solution resistance, but is related to the coating performance as well, with coating contributions predominant. The  $R_f$  and  $R_t$  curves are similar and appear to control  $R_{total}$ . The peaks in these curves at 12 days correlate with the small value of  $I_{CORR}$ . Also, the loss of resistance at 44 days is indicative of complete coating failure. This is supported by a high corrosion current (Fig. 20b) and by large values of capacitance, particularly  $C_c$  (Fig. 23), which remains very small and nearly constant up to day 44, then increases sharply. Extrapolation of the linear portion of the Bode magnitude curve to zero frequency indicates that the corrosion process is diffusion controlled up to about day 36, when coating breakdown allows acceleration of diffusion processes, and charge transfer becomes the controlling mechanism.

## Red Lead Oxide Primer With 0.7 Mils Topcoat

The polarization resistance data are shown in Figure 26. The  $I_{CORR}$  versus time curve shows that a fairly low corrosion current is maintained through day 45. After day 45 the corrosion current increases sharply, representing breakdown of the system. Comparison of the  $I_{CORR}$  versus time curves for topcoated systems shows that the oxide corrosion current is an order of magnitude smaller than that of the zinc. Since corrosion current is directly proportional to corrosion rate, it is obvious that the red lead

### OXIDE PRIMER

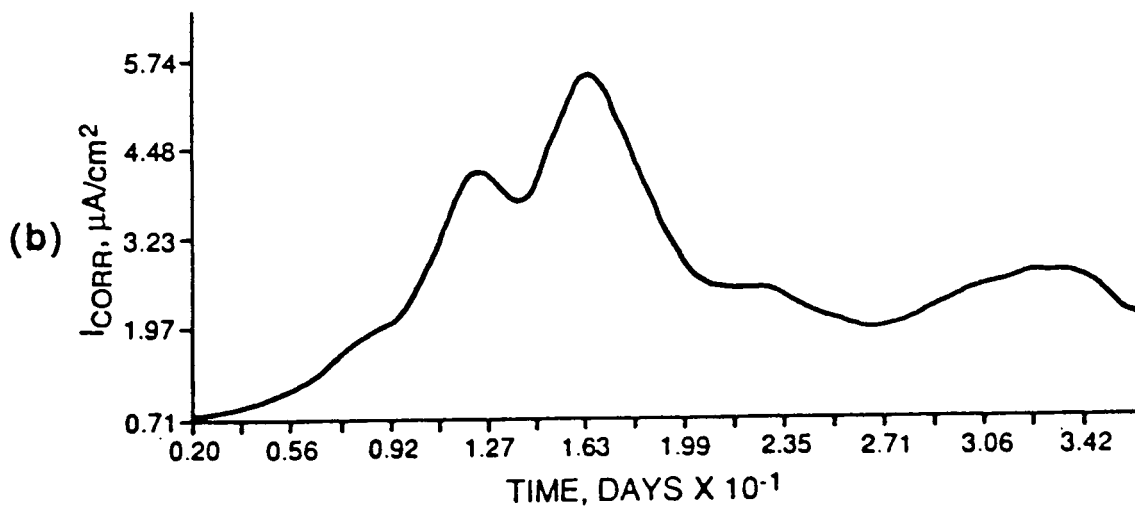
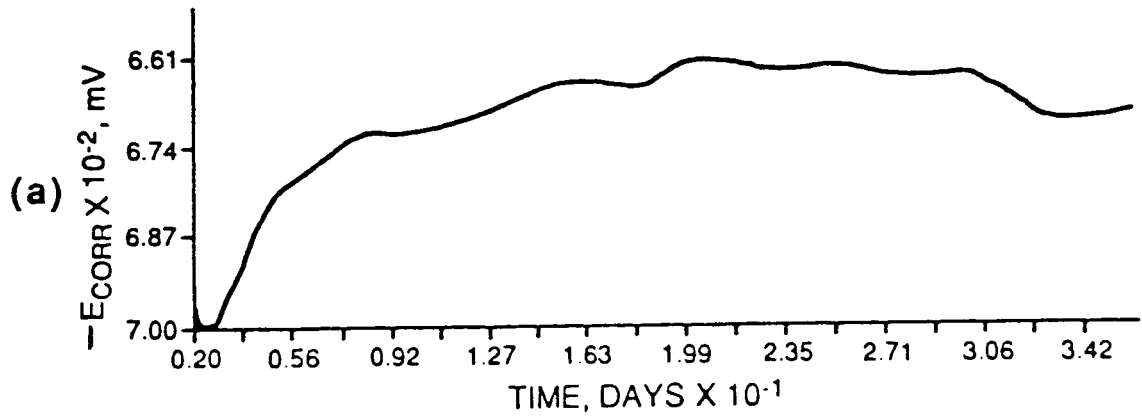


Figure 15.  $E_{CORR}$  and  $I_{CORR}$  versus time - red lead oxide primer.

### OXIDE PRIMER

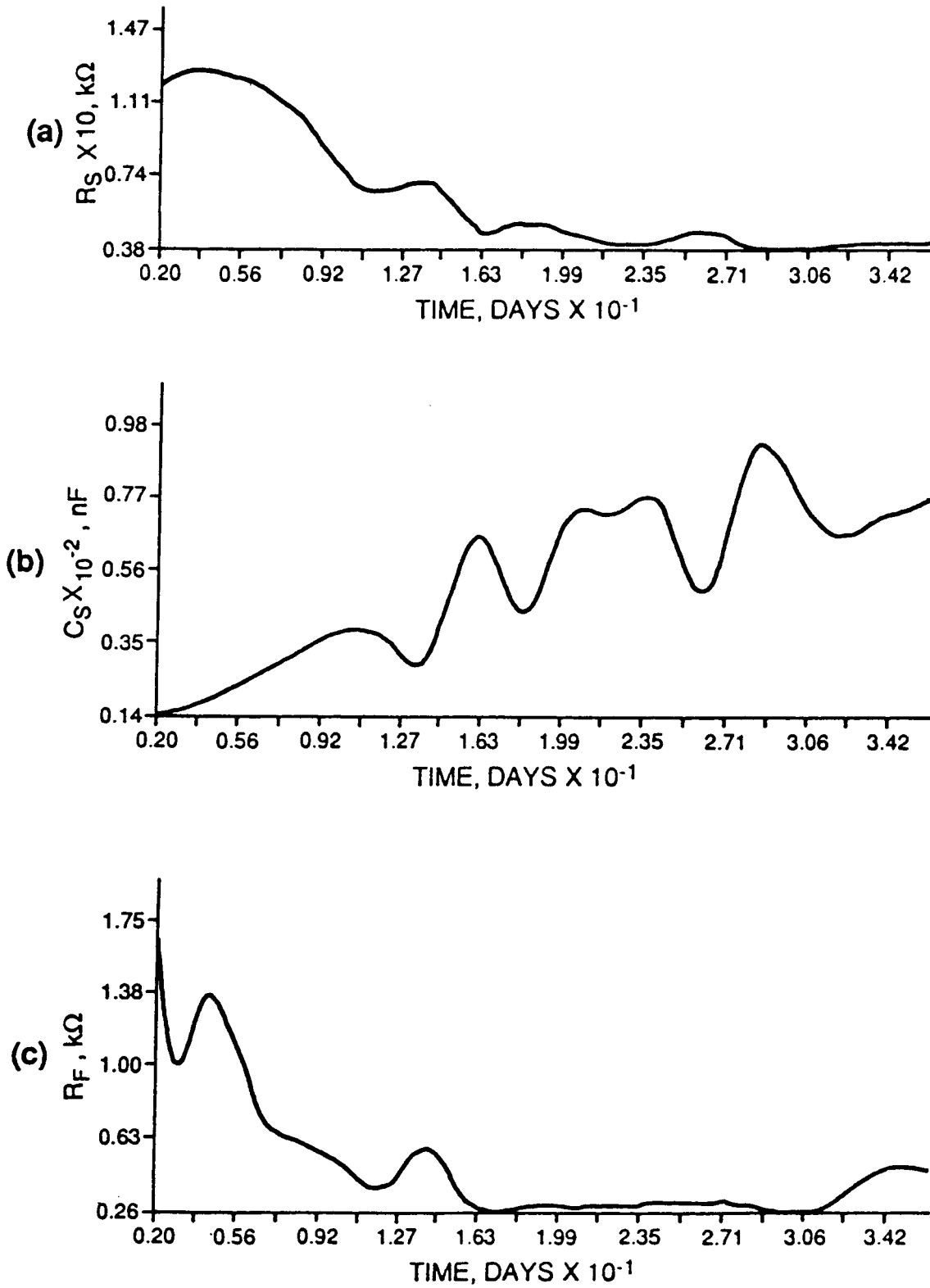


Figure 16.  $R_S$ ,  $C_S$ , and  $R_f$  versus time – red lead oxide primer.

### OXIDE PRIMER

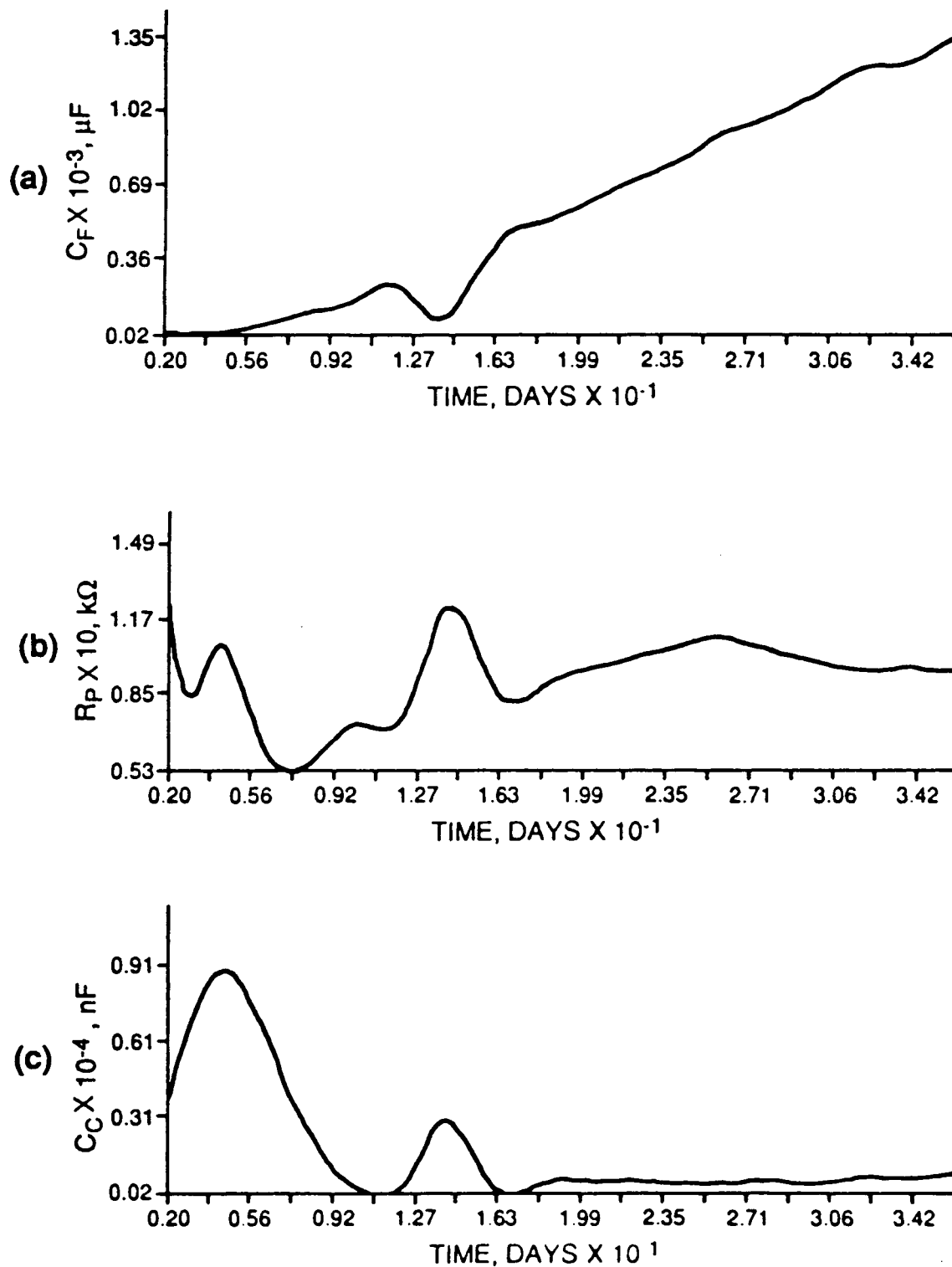


Figure 17.  $C_f$ ,  $R_p$ , and  $C_c$  versus time – red lead oxide primer.

### OXIDE PRIMER

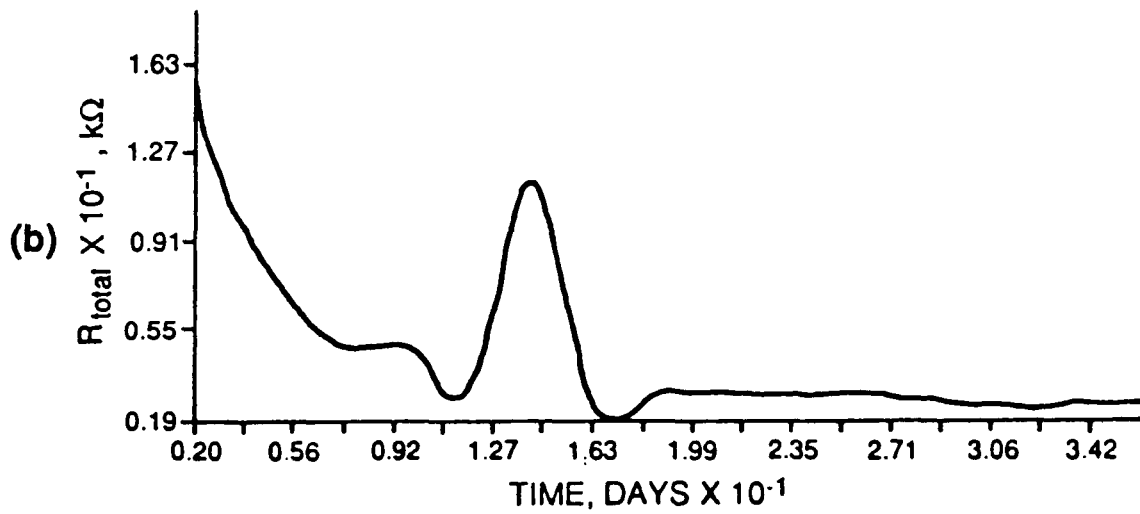
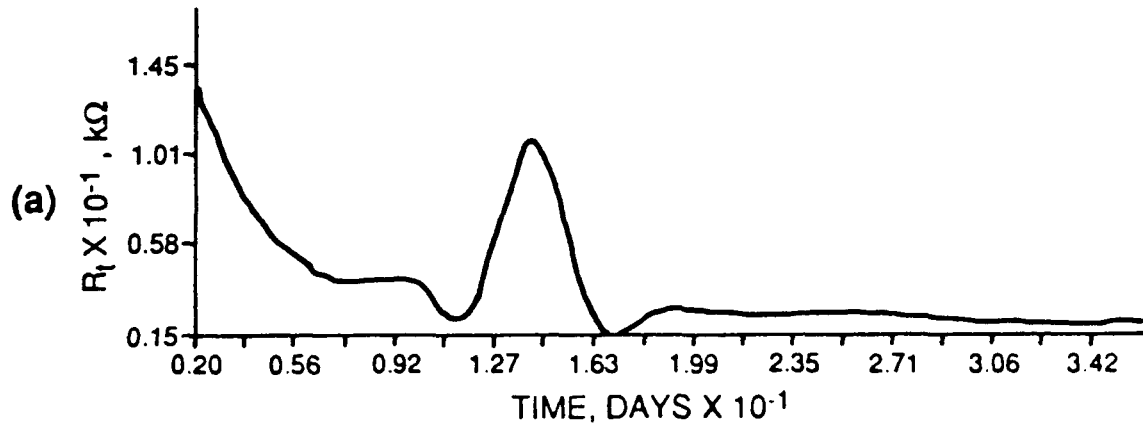


Figure 18.  $R_t$  and  $R_{total}$  versus time – red lead oxide primer.

### OXIDE PRIMER

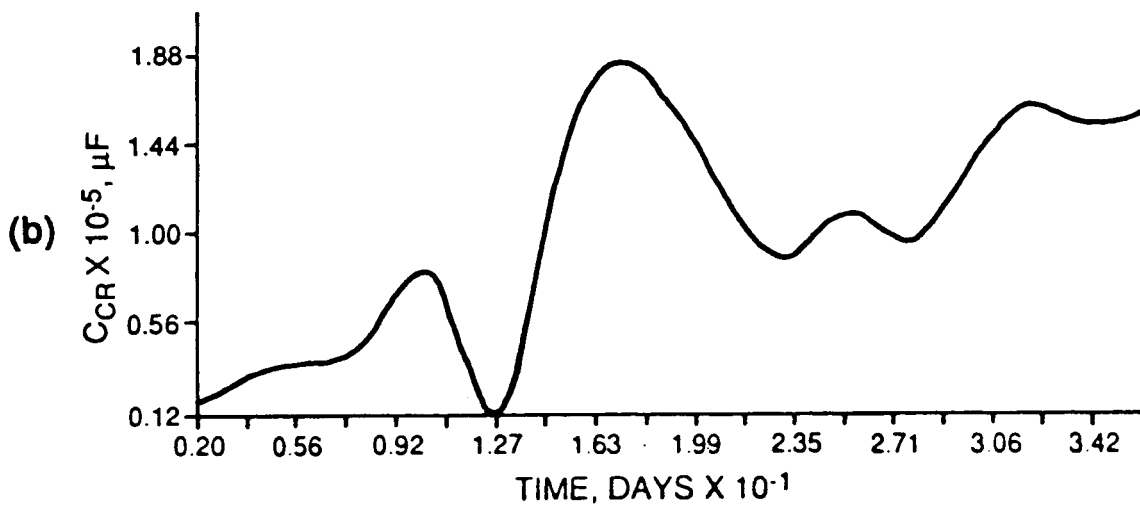
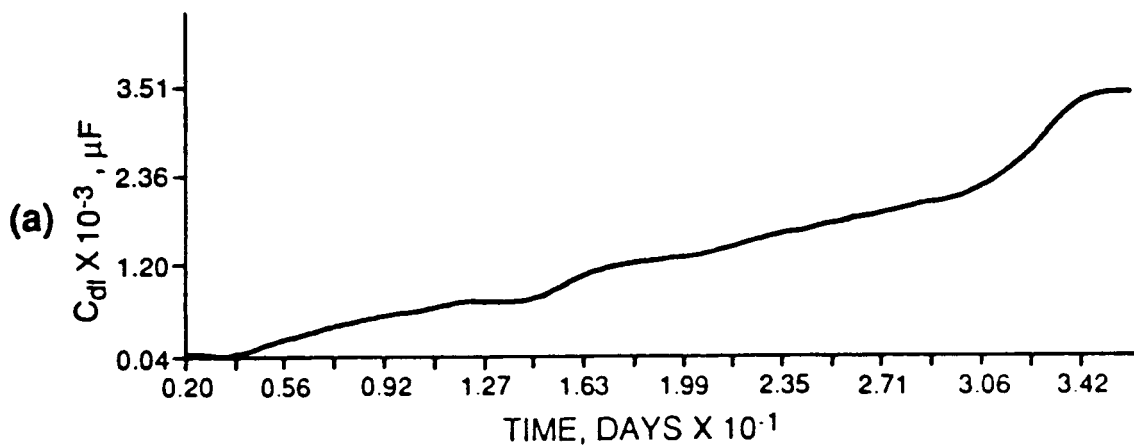


Figure 19.  $C_{dl}$  and  $C_{CR}$  versus time – red lead oxide primer.

ZINC RICH PRIMER  
0.7 MILS TOPCOAT

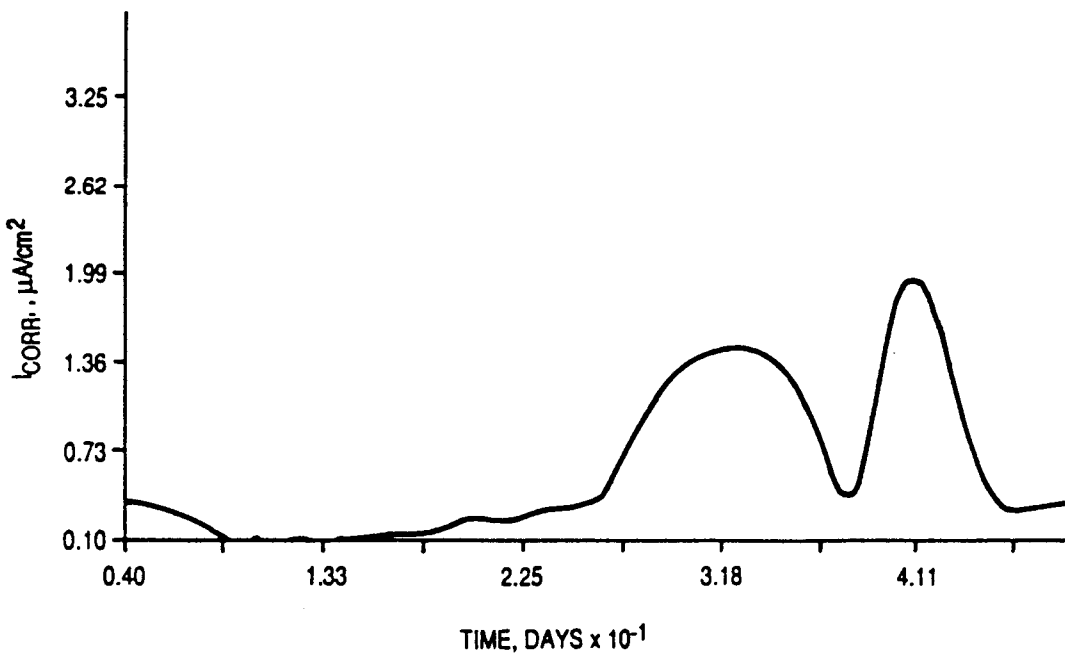
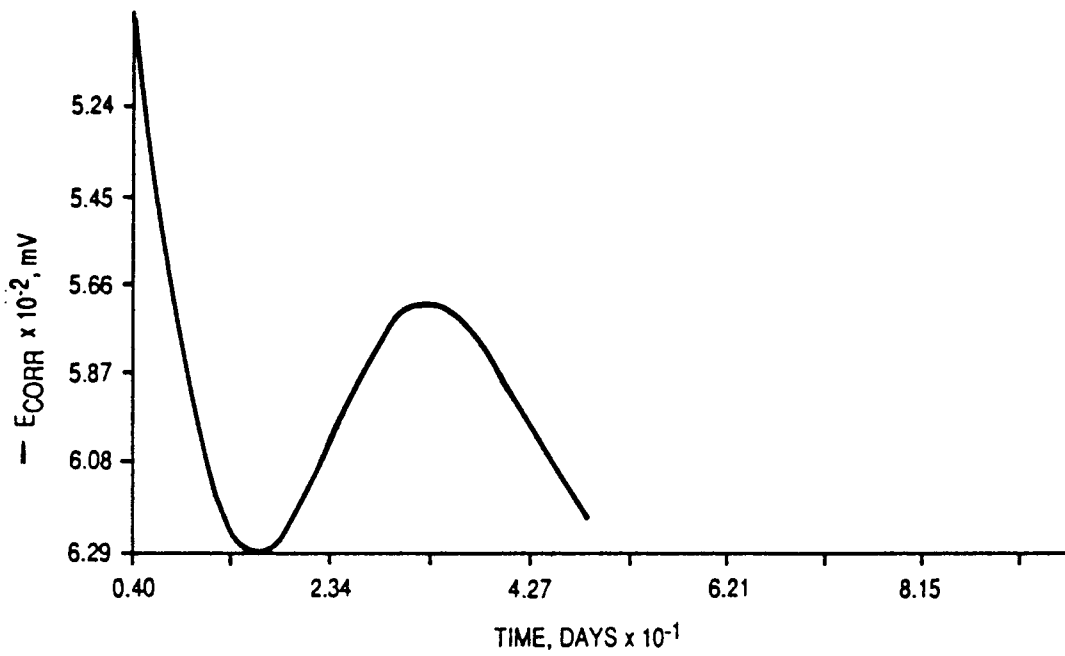


Figure 20.  $E_{CORR}$  and  $I_{CORR}$  versus time – zinc-rich primer + 0.7 mil topcoat.

ZINC RICH PRIMER  
0.7 MILS TOPCOAT

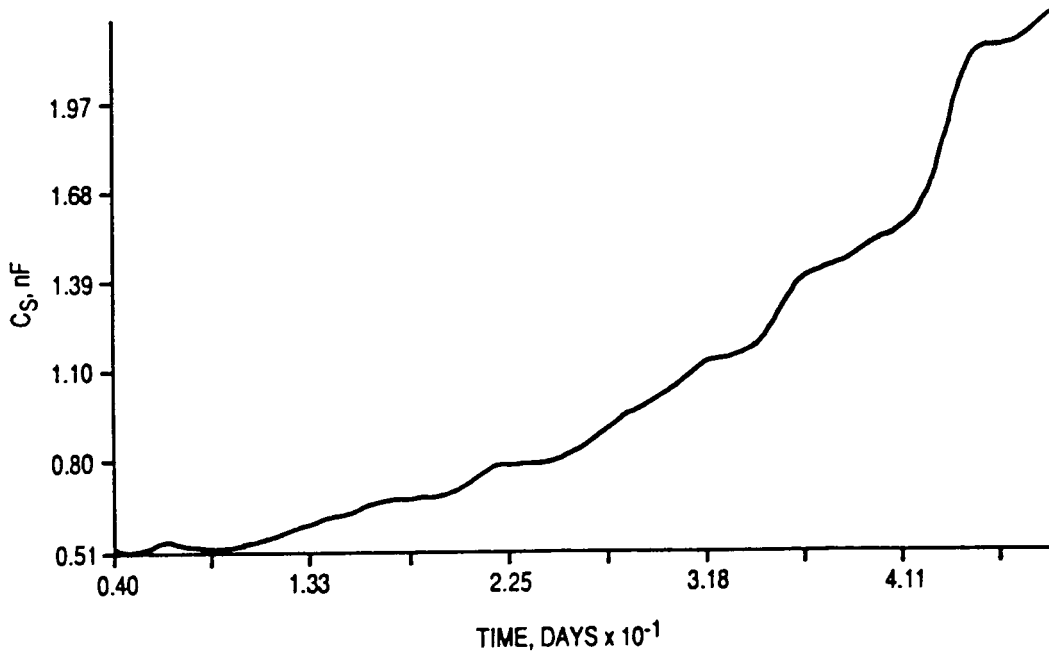
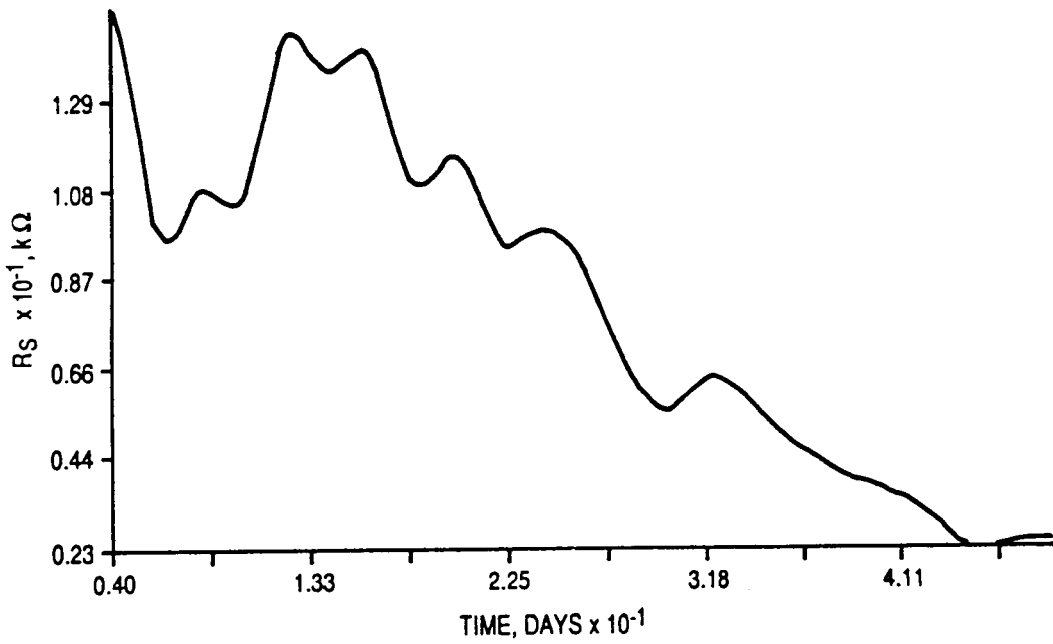


Figure 21.  $R_S$  and  $C_S$  versus time – zinc-rich primer + 0.7 mil topcoat.

ZINC RICH PRIMER  
0.7 MILS TOPCOAT

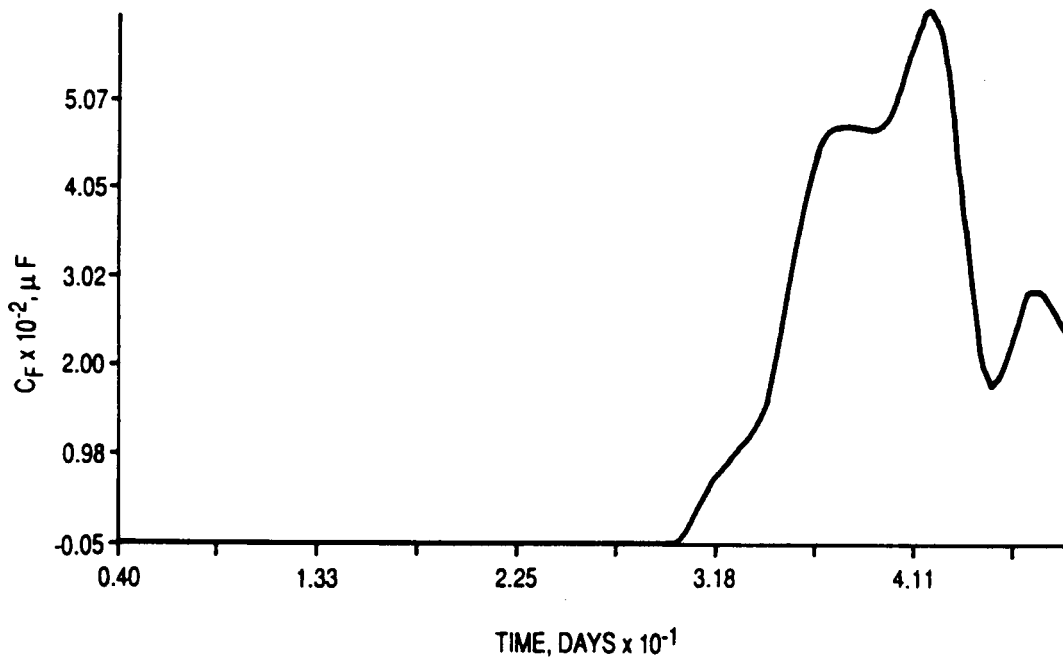
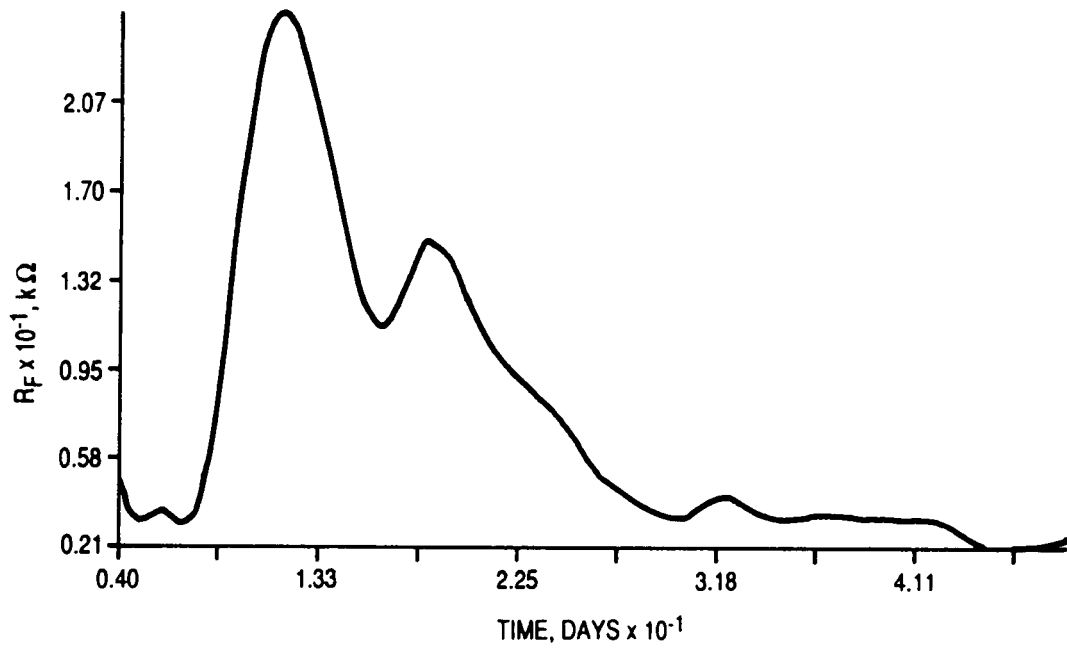


Figure 22.  $R_f$  and  $C_f$  versus time - zinc-rich primer + 0.7 mil topcoat.

**ZINC RICH PRIMER  
0.7 MILS TOPCOAT**

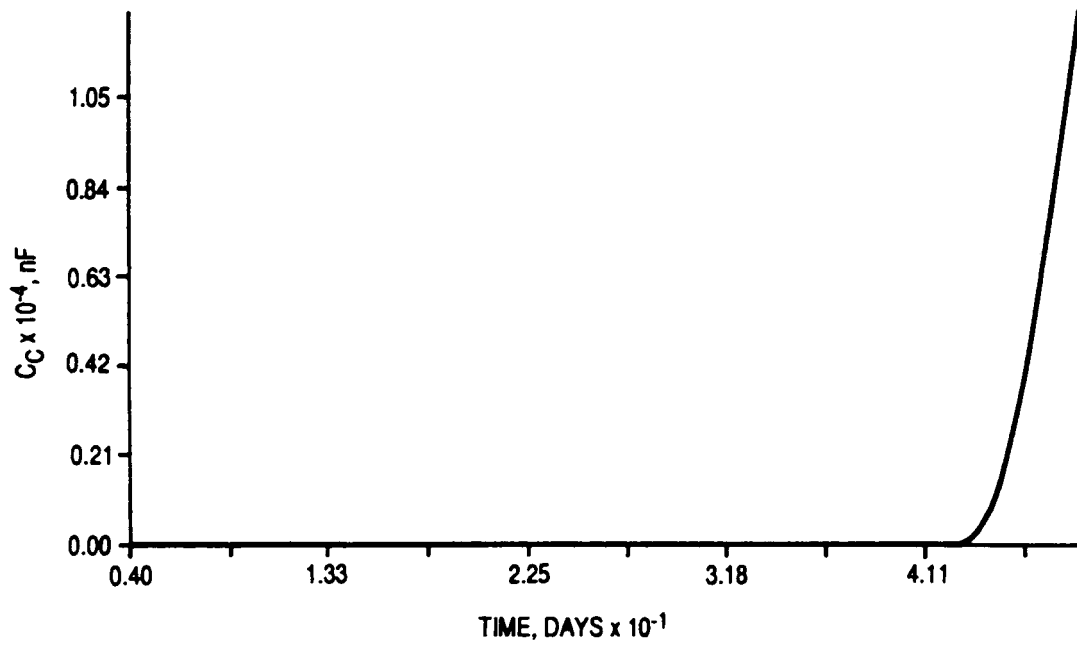
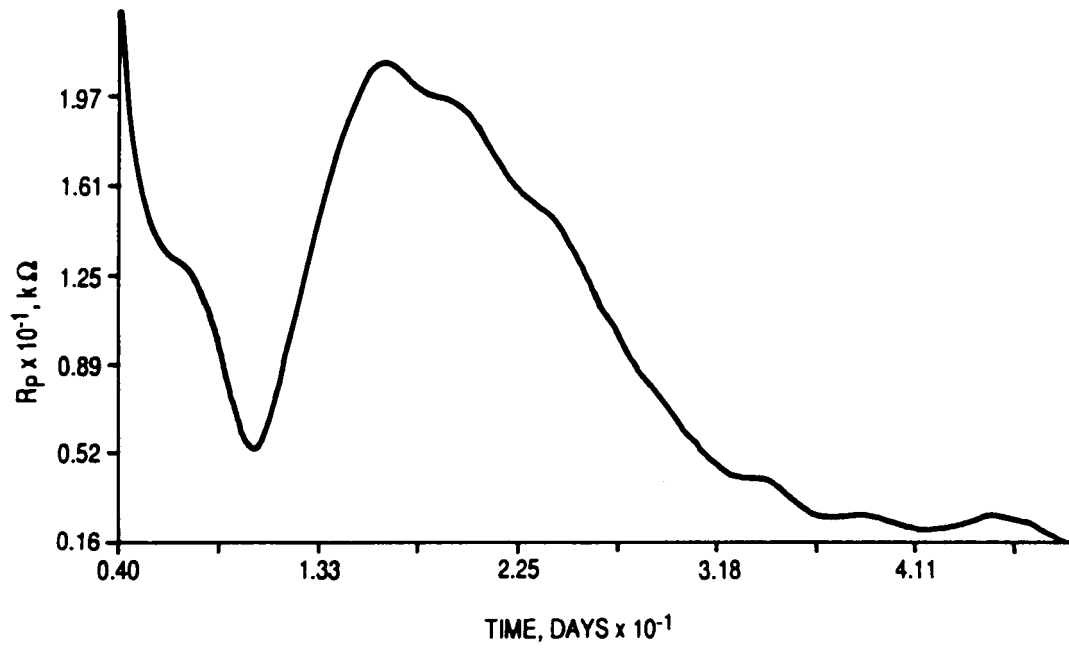


Figure 23.  $R_p$  and  $C_c$  versus time – zinc-rich primer + 0.7 mil topcoat.

**ZINC RICH PRIMER  
0.7 MILS TOPCOAT**

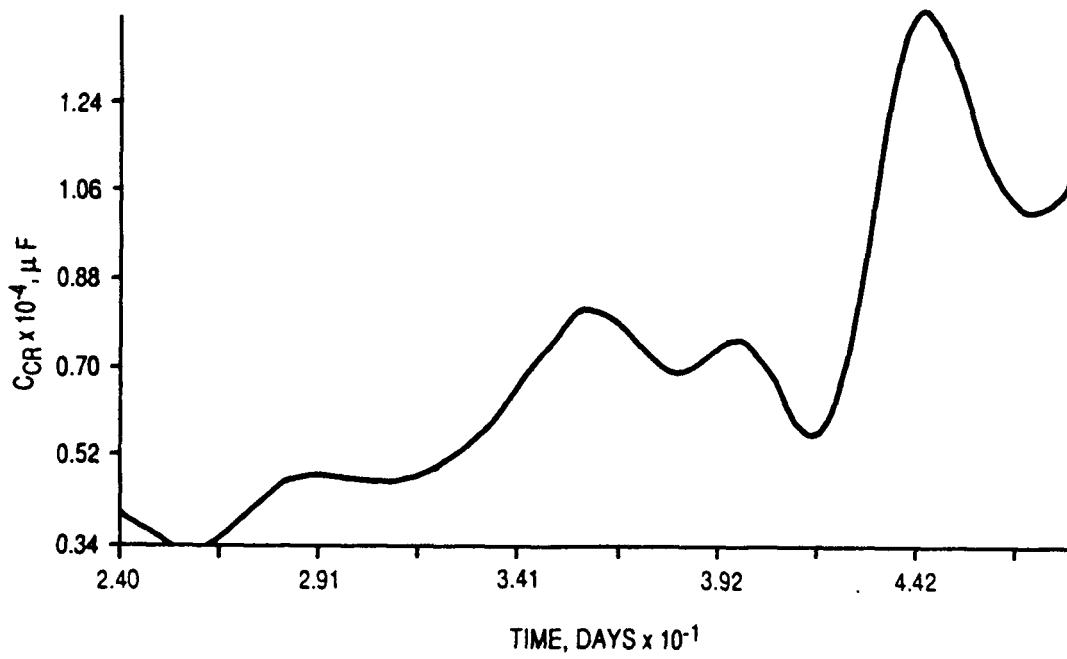
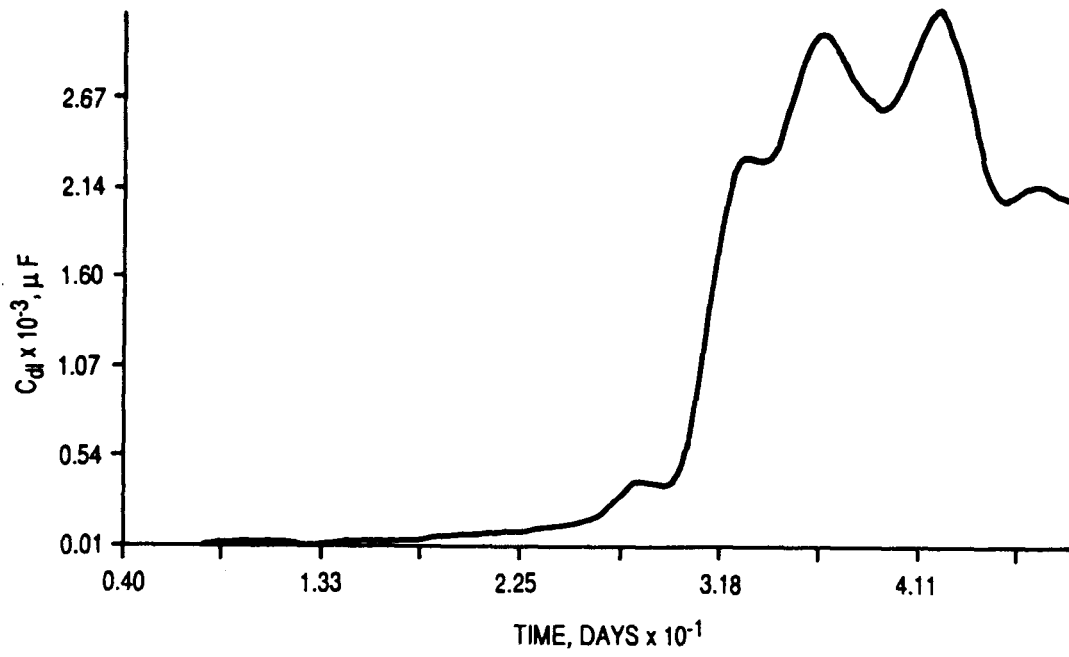


Figure 24.  $C_{dl}$  and  $C_{CR}$  versus time – zinc-rich primer + 0.7 mil topcoat.

**ZINC RICH PRIMER  
0.7 MILS TOPCOAT**

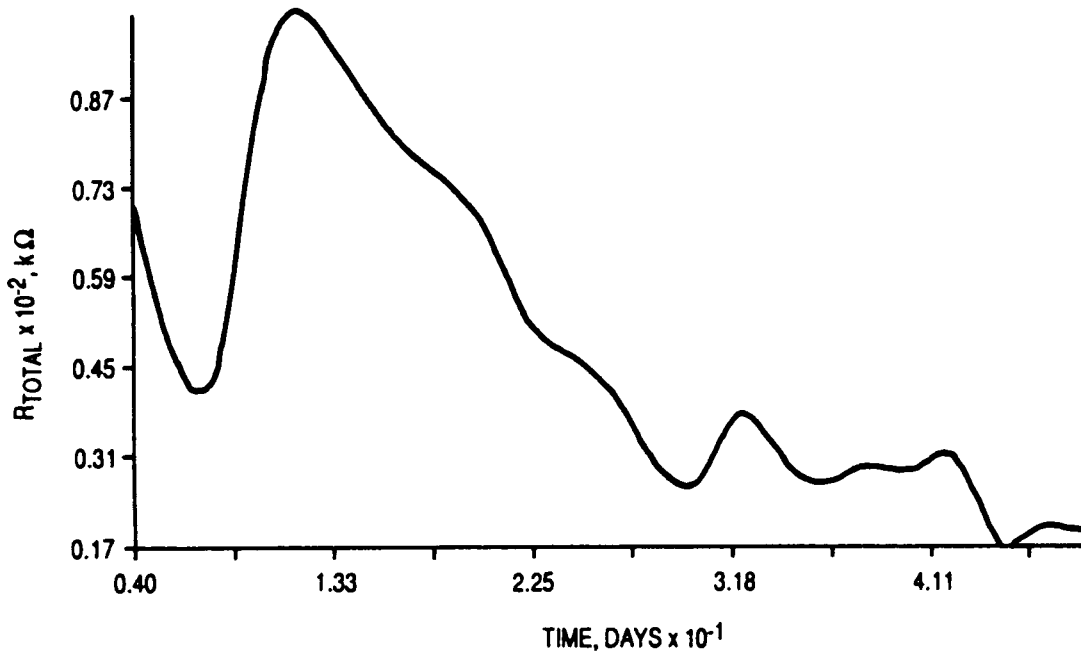
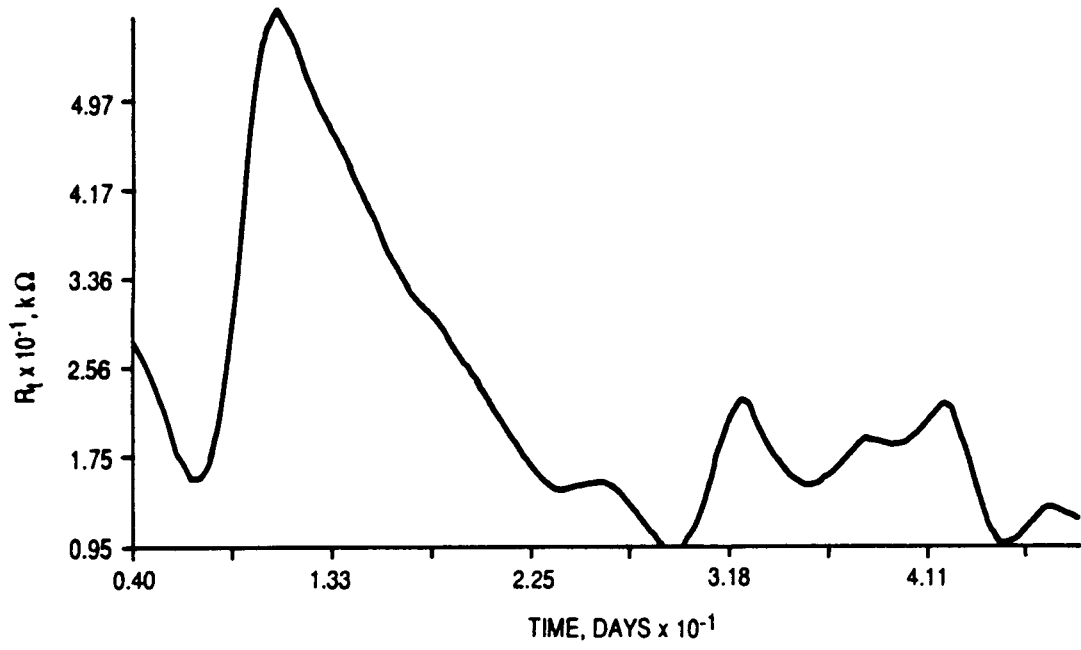


Figure 25.  $R_t$  and  $R_{total}$  versus time – zinc-rich primer + 0.7 mil topcoat.

**OXIDE PRIMER  
0.7 MILS TOPCOAT**

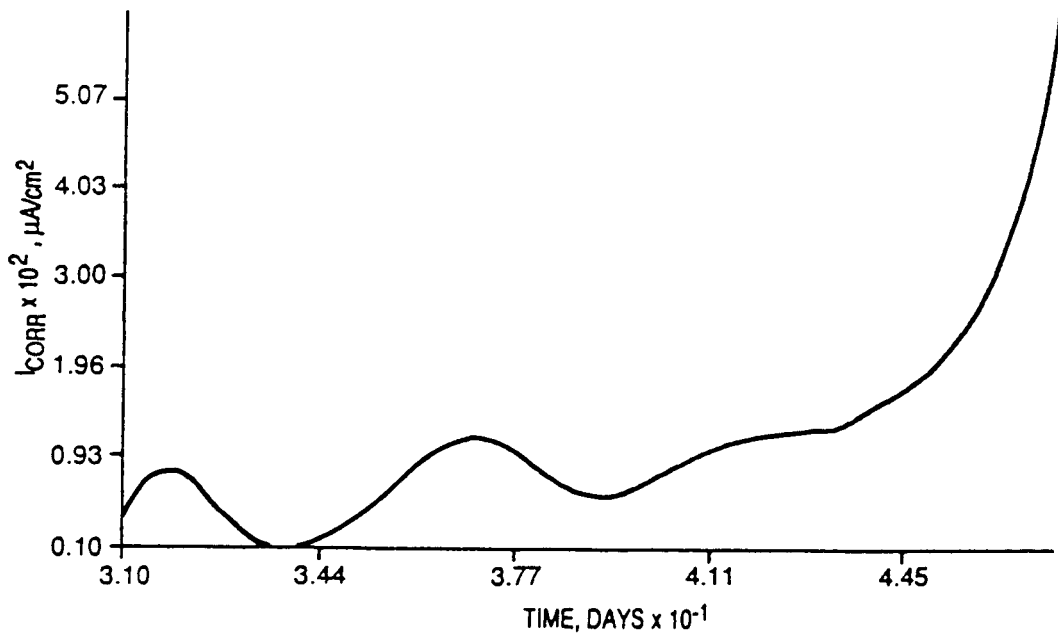
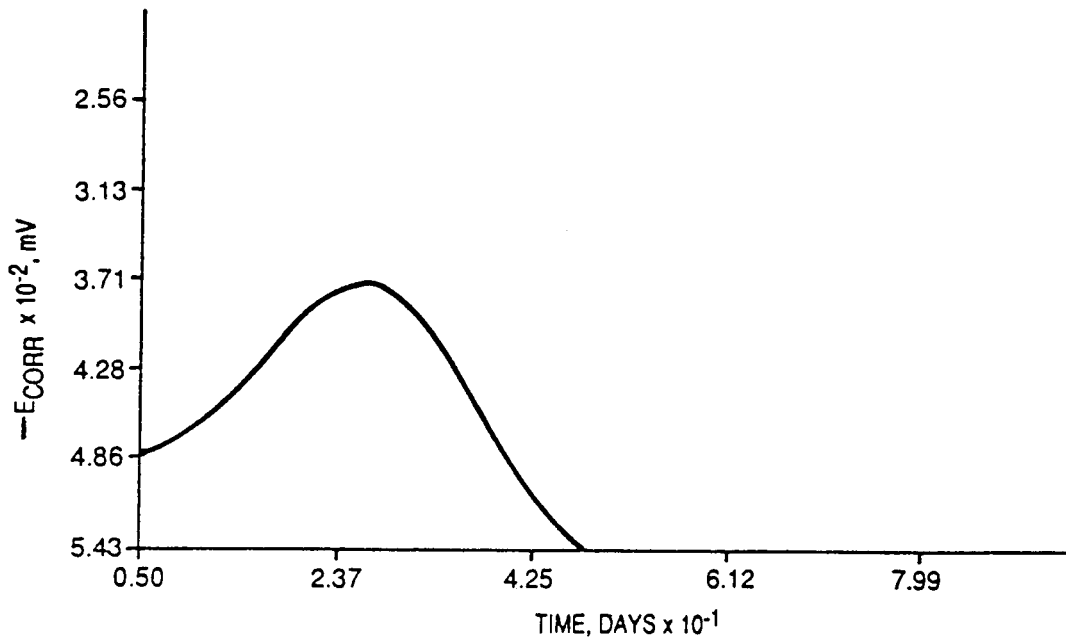


Figure 26.  $E_{CORR}$  and  $I_{CORR}$  versus time – red lead oxide primer + 0.7 mil topcoat.

oxide-topcoat system provides better protection than the zinc-rich primer system for this phase of experimentation. This is confirmed by the AC impedance data (Figs. 27 to 31). The value of the resistances for the red lead oxide-topcoat system are two to three orders of magnitude greater than the zinc-rich topcoat system, while the values of the capacitances are two to four orders of magnitude smaller. Both of these factors contribute to the large differences in impedance as illustrated by comparing Figures 5 and 6.

AC impedance data were analyzed using the equivalent circuit in Figure 2. The equivalent circuit in Figure 4 was not used because the least squares program would not converge given the starting parameters. It was later discovered that the initial estimate for  $C_{CR}$  was too large each time the least-squares program was run using the model of Figure 4, and that a smaller estimate would have resulted in convergence.

The AC impedance data for this system are typical in most respects. The resistance versus time curves are all decreasing, reaching a minimum value at about 45 days. Again, the total resistance is controlled by the two charge resistances,  $R_t$  and  $R_f$ . The  $C_{dl}$  and  $C_f$  curves increase drastically at 45 days. (These results confirm failure of the system as predicted by the DC data.) The  $C_c$  versus time curve (Fig. 29), however, falls to a minimum value at 45 days, representing an increase in impedance. This may be due to the integrity of the primer-topcoat bond, which appears to remain intact even though the system as a whole is failing, probably at the metal-primer interface.

Extrapolation of the Bode magnitude plot to zero frequency indicates diffusion control during the entire immersion time. This is in contrast to the zinc-rich system, which showed charge transfer control at later immersion times, probably due to failure at the primer-topcoat interface.

### Zinc-Rich Primer With 2.3 Mils Topcoat

The  $E_{CORR}$  and  $I_{CORR}$  versus time curves are shown in Figure 32. The  $E_{CORR}$  versus time curve is generally increasing, while the  $I_{CORR}$  versus time curve shows no particular trend. This lack of shape is probably due to the thickness of the coating system. Thicker coating systems generally provide greater corrosion protection resulting in lower values of corrosion current density (compare Fig. 32 with Fig. 20). There is a tolerance limit below which the DC polarization resistance technique is ineffective. This system appears to have reached (or is close to) that limit. The AC impedance technique, however, is much more sensitive than the DC technique. Thus, the AC impedance technique can be used effectively to evaluate the performance of thicker coating systems.

AC impedance data are shown in Figures 33 to 36. Note the change in parameter values toward much greater impedance values as compared to the system with 0.7 mils topcoat. In general, resistance versus time curves are decreasing. Again, the total resistance appears to be controlled by  $R_t$  and  $R_f$ , as illustrated in Figure 35. Figure 35 also shows the  $I_{CORR}$  versus time curve as determined using impedance data.  $I_{CORR}$  is calculated from the Stern-Geary equation for charge transfer control [7-9], using estimated Tafel constants (50 mV each for  $b_a$  and  $b_c$ ) and  $(R_t + R_f)$  as the total charge transfer resistance:

$$I_{CORR} = \frac{b_a b_c}{2.303 (b_a + b_c)} \cdot \frac{1}{R_t} \quad (1)$$

OXIDE PRIMER  
0.7 MILS TOPCOAT

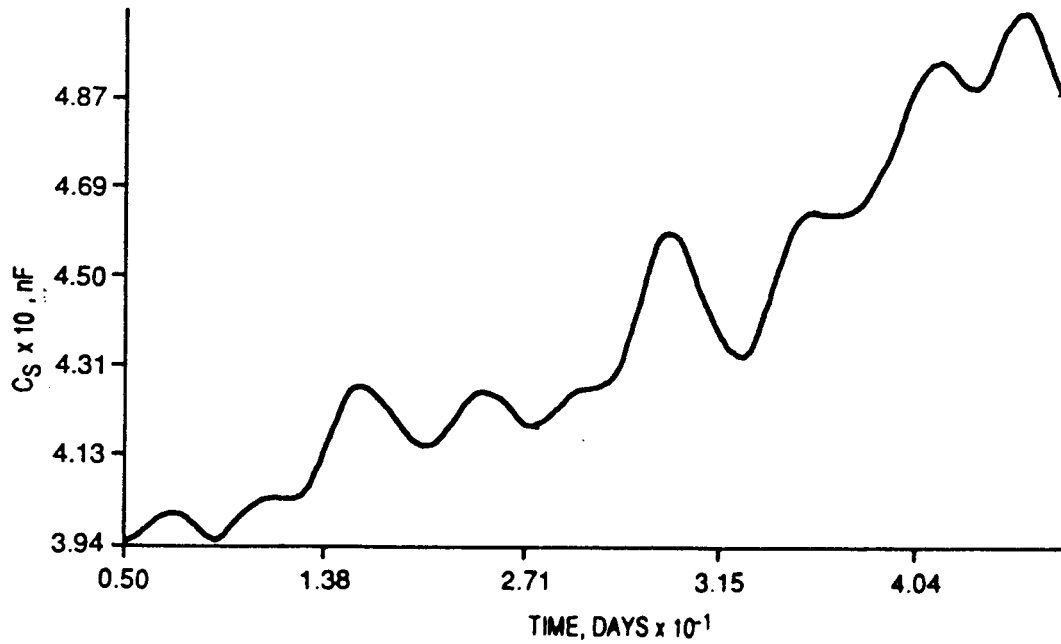
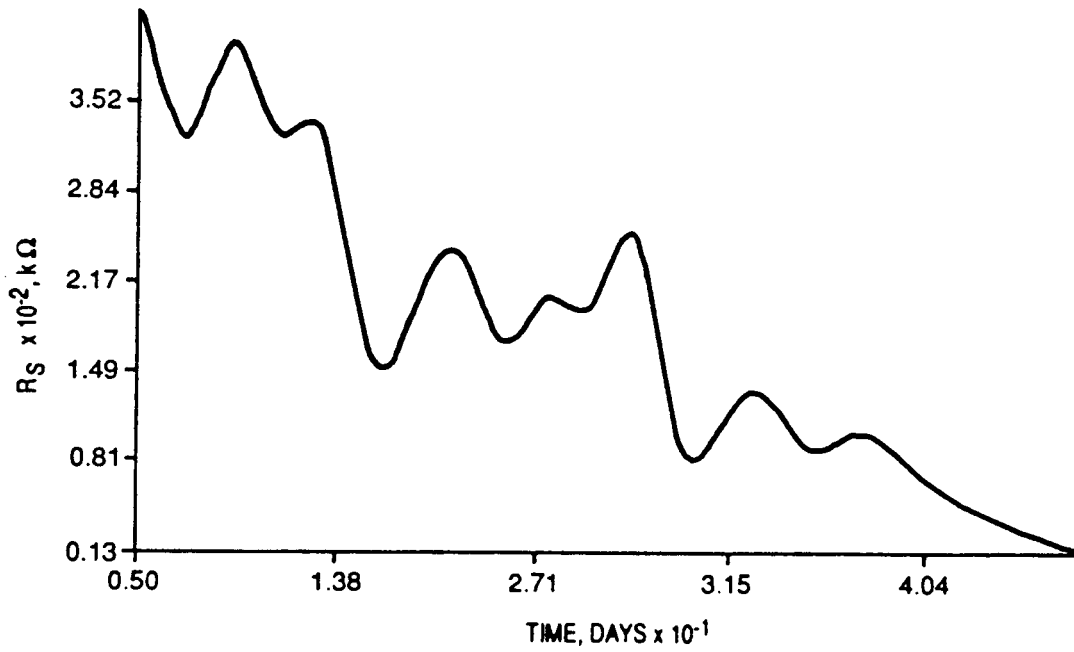


Figure 27.  $R_S$  and  $C_S$  versus time – red lead oxide primer + 0.7 mil topcoat.

OXIDE PRIMER  
0.7 MILS TOPCOAT

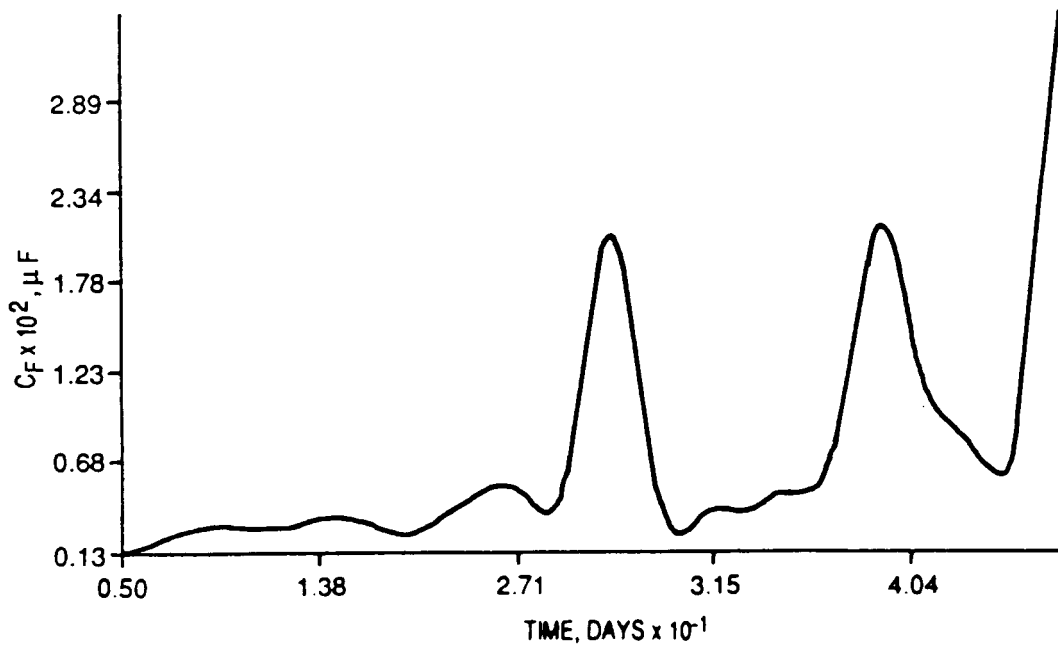
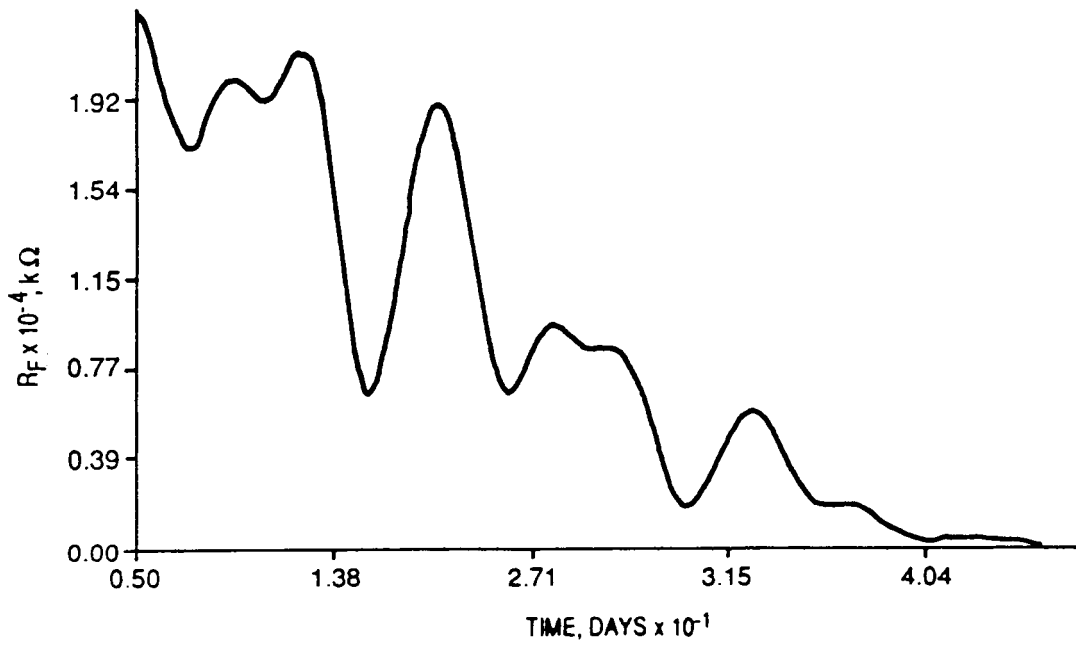


Figure 28. R<sub>f</sub> and C<sub>F</sub> versus time – red lead oxide primer + 0.7 mil topcoat.

**OXIDE PRIMER  
0.7 MILS TOPCOAT**

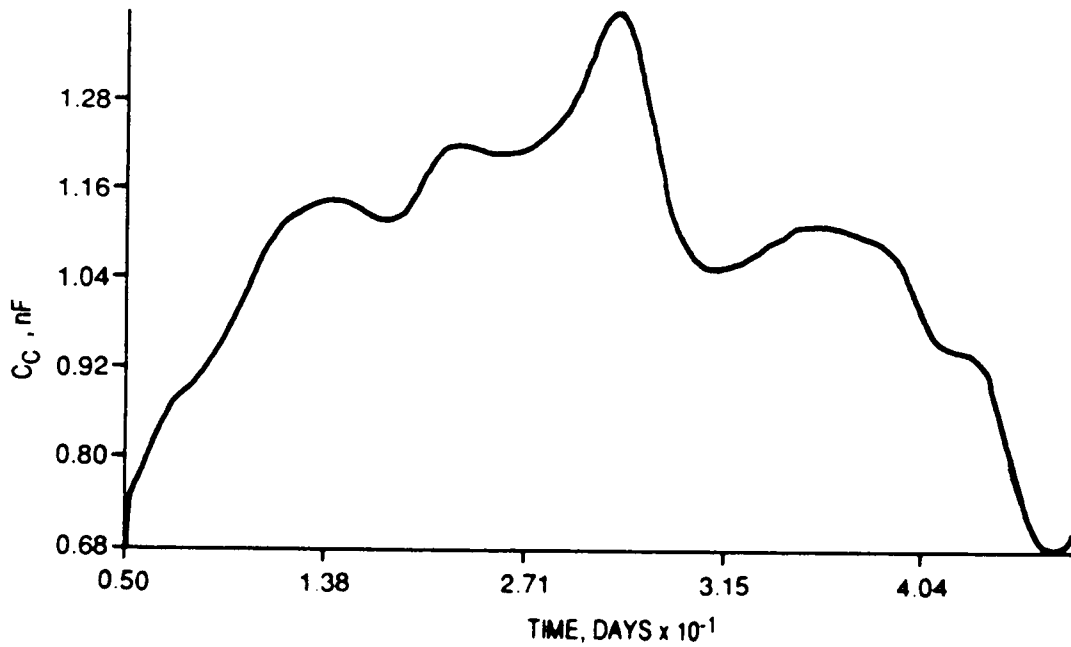
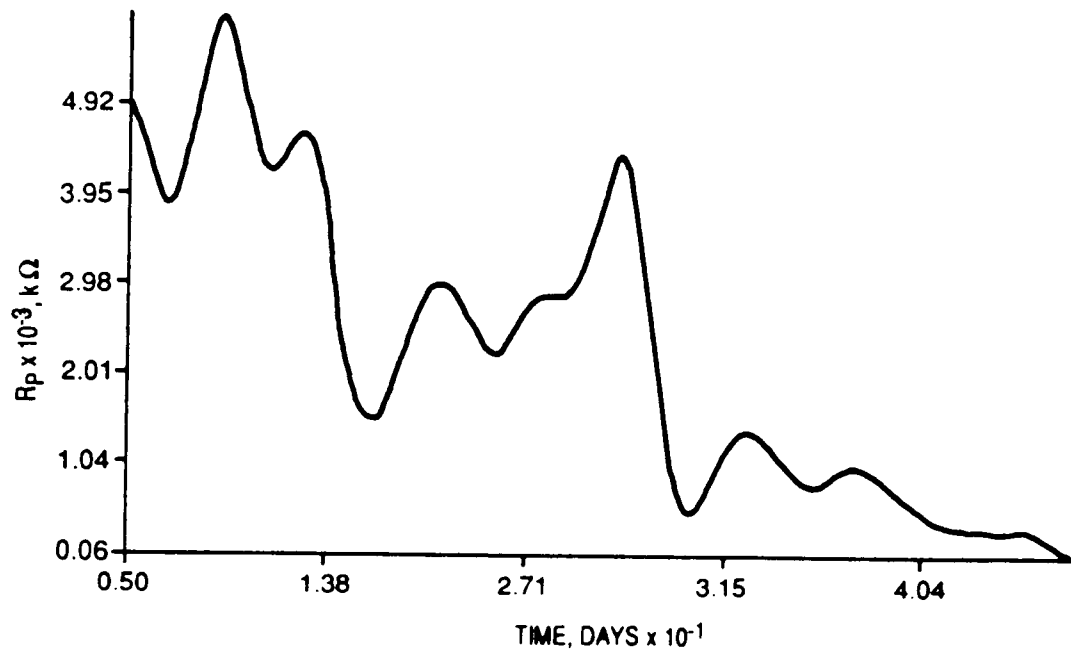


Figure 29.  $R_p$  and  $C_c$  versus time – red lead oxide primer + 0.7 mil topcoat.

**OXIDE PRIMER  
0.7 MILS TOPCOAT**

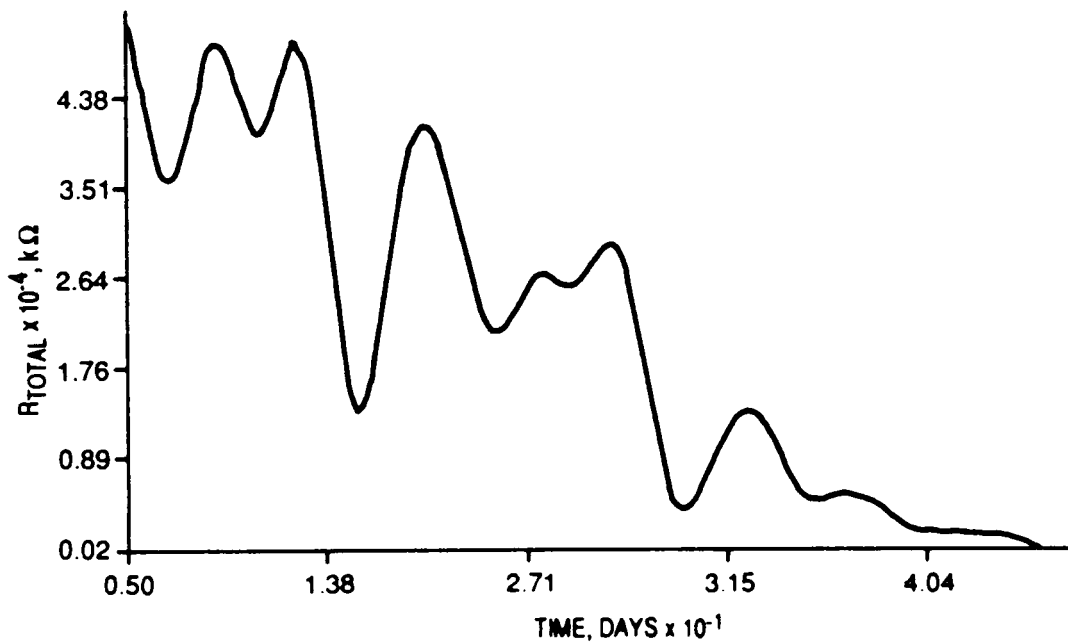
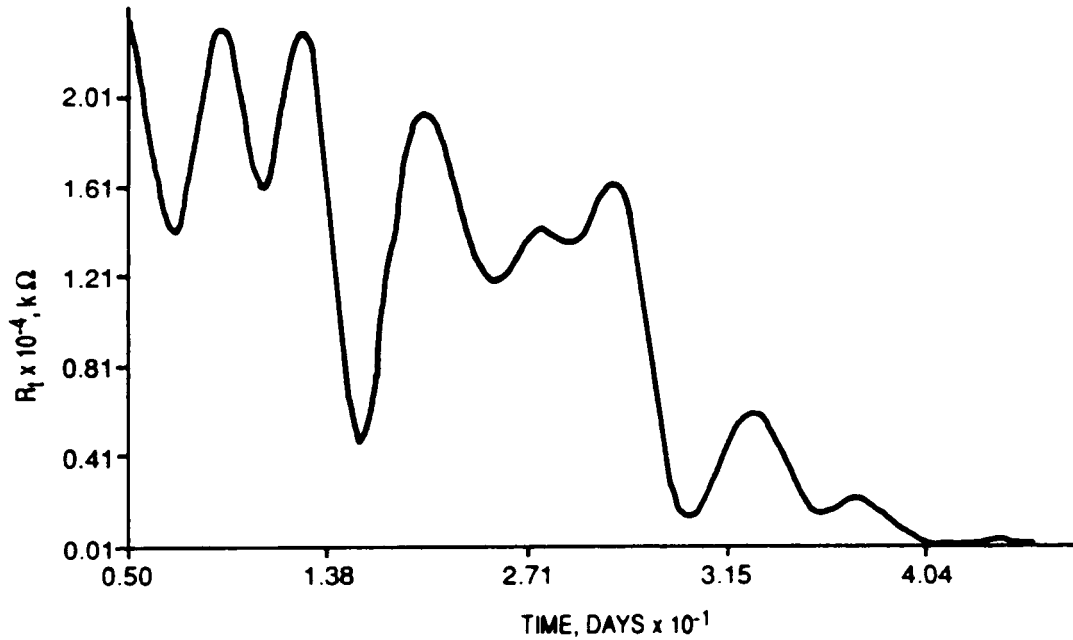


Figure 30.  $R_t$  and  $R_{total}$  versus time - red lead oxide primer + 0.7 mil topcoat.

**OXIDE PRIMER  
0.7 MILS TOPCOAT**

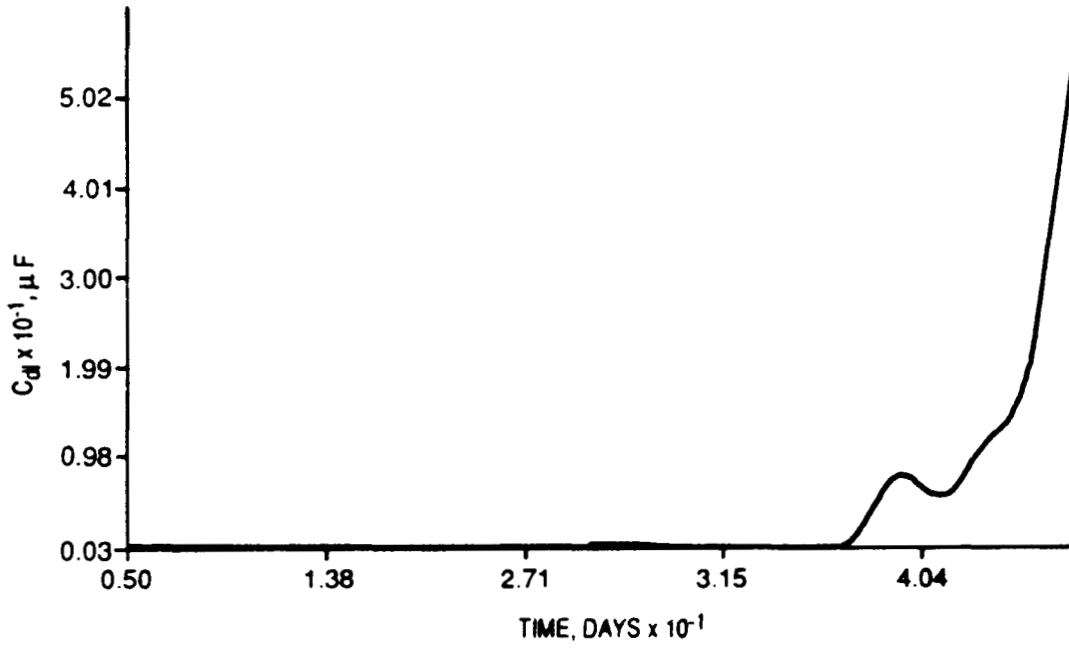


Figure 31.  $C_{dl}$  versus time – red lead oxide primer + 0.7 mil topcoat.

ZINC RICH PRIMER  
2.3 MILS TOPCOAT

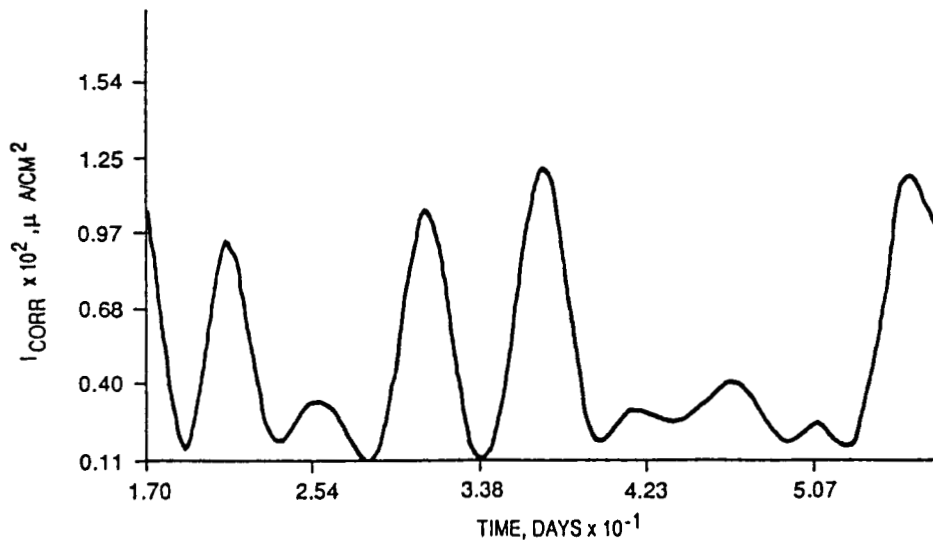
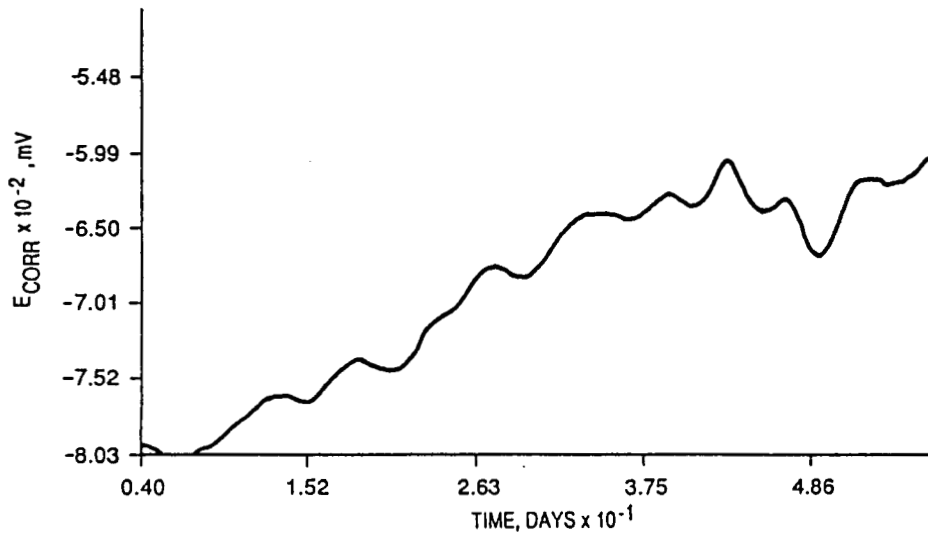


Figure 32.  $E_{CORR}$  and  $I_{CORR}$  versus time - zinc-rich primer + 2.3 mils topcoat.

ZINC RICH PRIMER  
2.3 MILS TOPCOAT

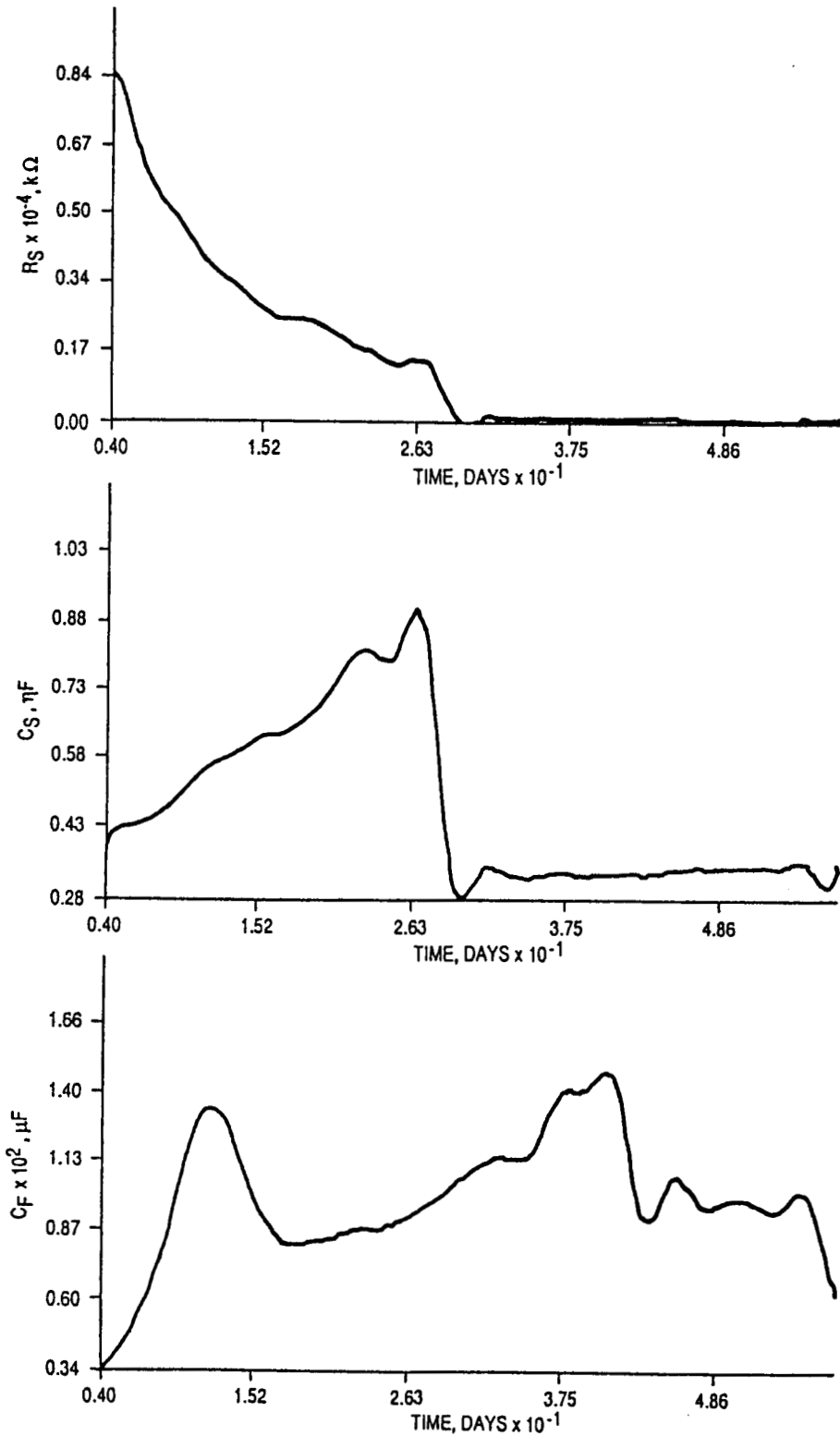


Figure 33.  $R_S$ ,  $C_S$ , and  $C_F$  versus time – zinc-rich primer + 2.3 mils topcoat.

ZINC RICH PRIMER  
2.3 MILS TOPCOAT

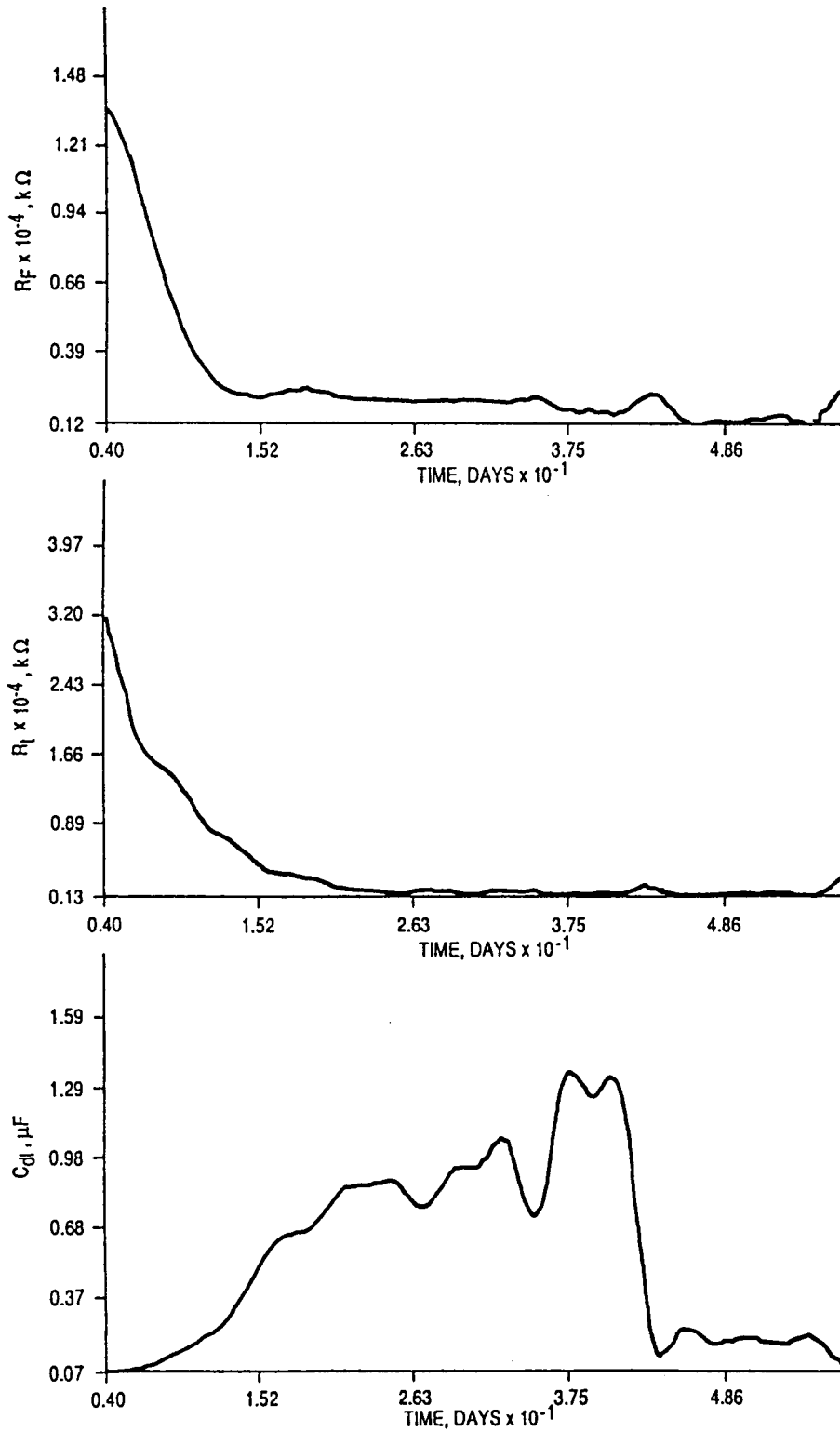


Figure 34.  $R_f$ ,  $R_t$ , and  $C_{dl}$  versus time – zinc-rich primer + 2.3 mils topcoat.

ZINC RICH PRIMER  
2.3 MILS TOPCOAT

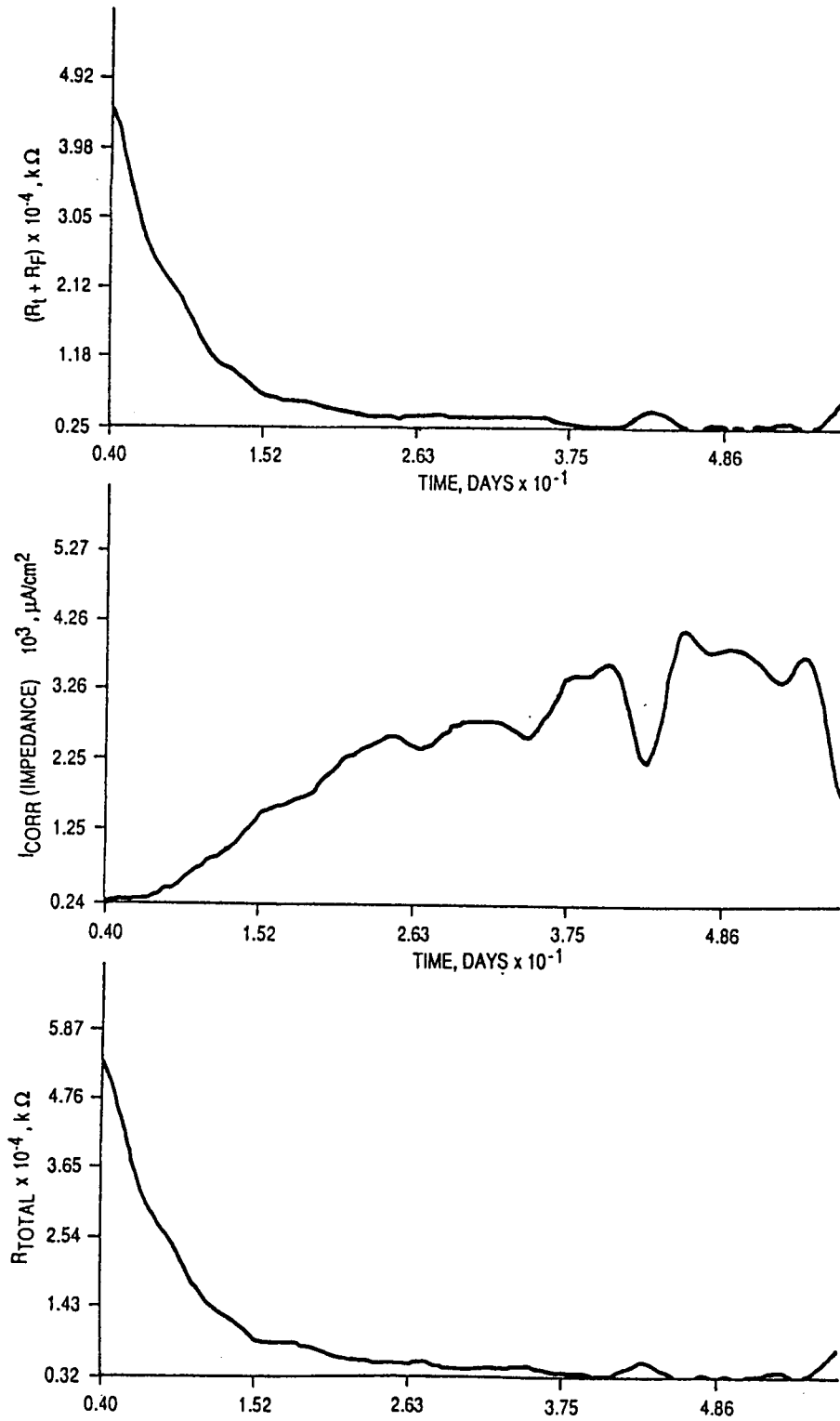


Figure 35.  $(R_t + R_f)$ ,  $I_{CORR}$  (impedance), and  $R_{total}$  versus time – zinc-rich primer  
× 2.3 mils topcoat.

ZINC RICH PRIMER  
2.3 MILS TOPCOAT

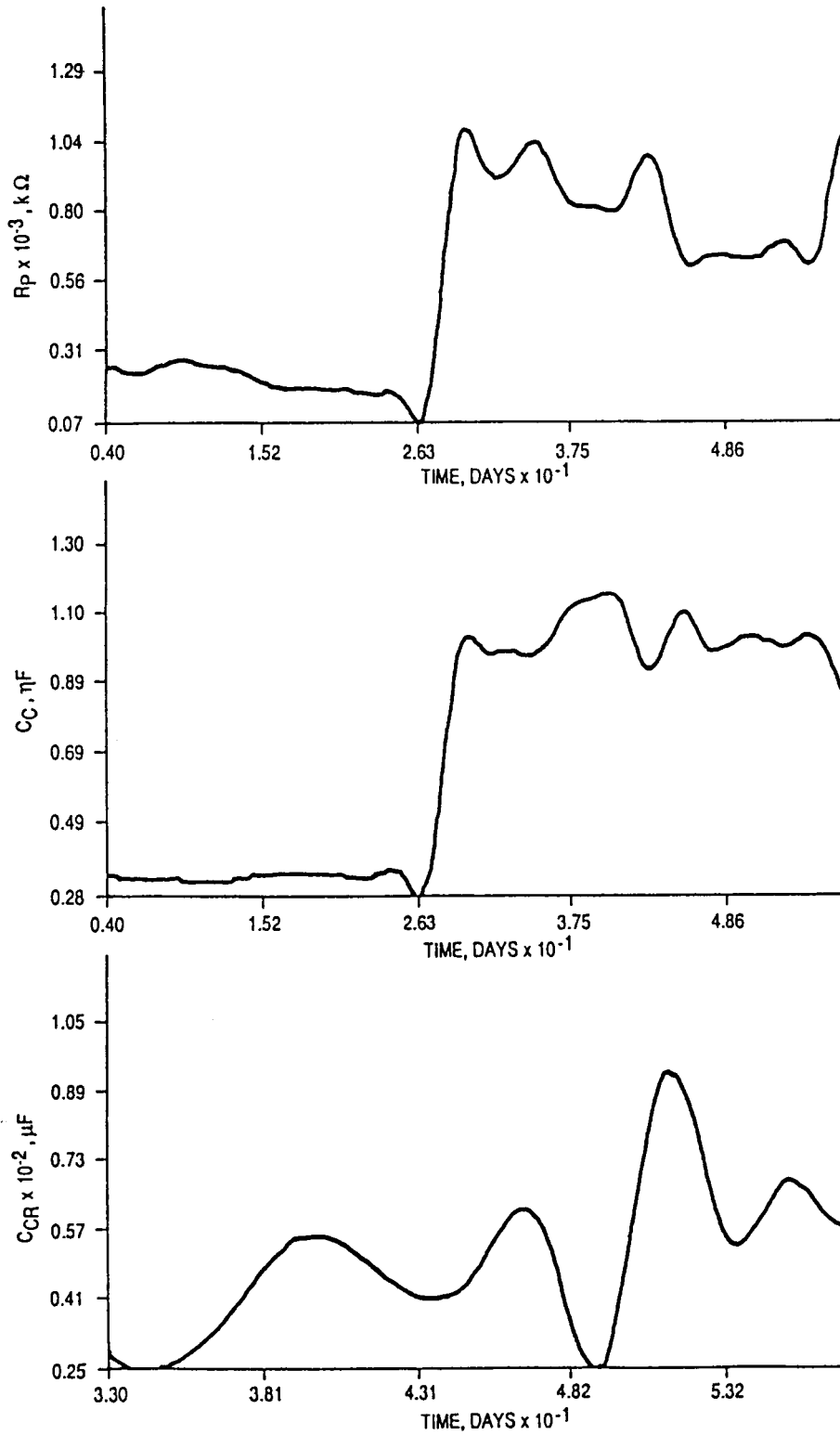


Figure 36. R<sub>p</sub>, C<sub>c</sub>, and C<sub>CR</sub> versus time – zinc-rich primer + 2.3 mils topcoat.

where

$b_a$  = anodic Tafel slope

$b_c$  = cathodic Tafel slope

$R_t$  = charge transfer resistance .

The meaning and use of Tafel constants have been described previously [6]. The shape of this curve is consistent with changes in the other elements of the equivalent circuit. For example, the gradual increase in the  $C_{dl}$  versus time curve (Fig. 34) followed by a sudden decrease at 43 days corresponds to a gradual increase in  $I_{CORR}$  followed by a minimum at 43 days. Similar features are observed in the  $C_f$  versus time curve.

Extrapolation of the linear portion of the Bode magnitude plot to  $W = 0$  indicates that diffusion processes are controlling the corrosion rate at all times.

### **Red Lead Oxide Primer With 2.6 Mil Topcoat**

The polarization resistance data are shown in Figure 37. The  $E_{CORR}$  versus time curve is generally decreasing, while the  $I_{CORR}$  versus time curve shows the same lack of structure as does the zinc-rich system. These curves are of little use except to show that the corrosion rate is low.

The AC impedance data are shown in Figures 38 to 41. The  $R_S$  versus time curve (Fig. 38) shows that this element represents the largest of the single resistive elements and is comparable to the total charge transfer resistance curve,  $R_t + R_f$ . Clearly the shape and magnitude of this curve show that  $R_S$  does not represent the resistance of the solution, but is intimately associated with the paint system. The corrosion process is controlled by diffusion, as confirmed by extrapolation of the linear portion of the Bode magnitude plot to  $W = 0$ .

Figure 41b shows the  $I_{CORR}$  versus time curve calculated with impedance data using equation (1). The corrosion current rises very slowly and is virtually constant between 24 and 54 days at about  $0.0034 \mu A/cm^2$ . For 4130 steel, this corresponds to 0.0015 mils per year, which indicates very good protection, and is comparable to that for the thick zinc-rich primer-topcoat system.

The other time-dependent curves offer little for interpretation. The resistance curves are generally decreasing, but usually stabilize after about 21 days. The capacitance curves show no trend. This is due to the lack of coating failure, even after 60 days. (Figure 23b shows how capacitance can be affected by coating failure.)

### **Comparison of AC Impedance and the DC Methods for Obtaining Corrosion Rates**

The method of estimating corrosion rates using the DC polarization resistance technique is well known. The corrosion rate in mils per year (mpy) is related to the corrosion current density through the following equation:

OXIDE PRIMER  
2.6 MILS TOPCOAT

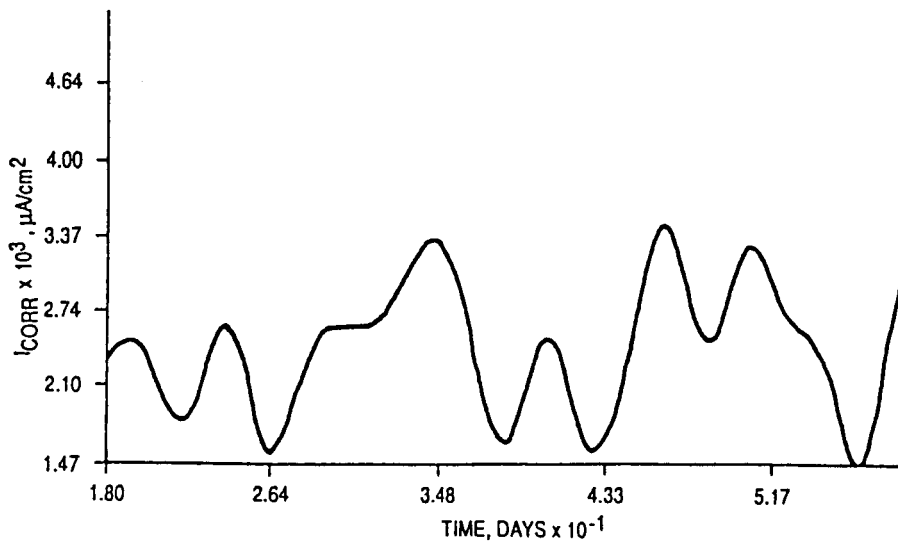
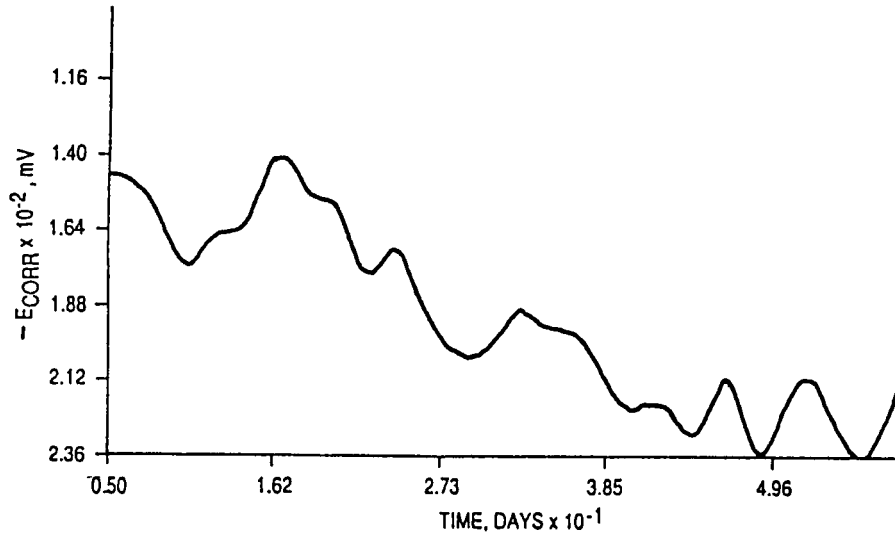


Figure 37.  $E_{CORR}$  and  $I_{CORR}$  versus time – red lead oxide primer + 2.6 mils topcoat.

OXIDE PRIMER  
2.6 MILS TOPCOAT

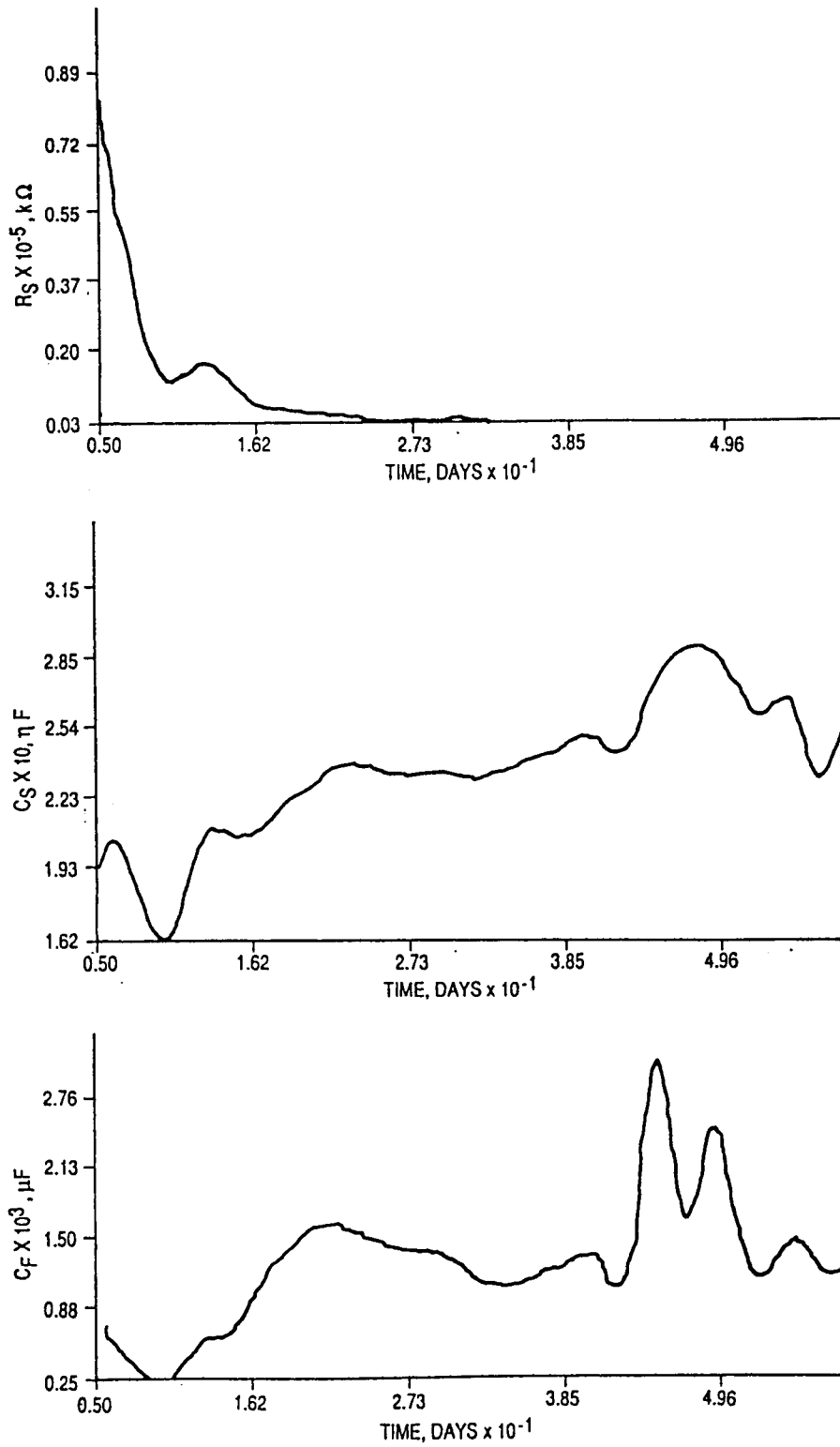


Figure 38.  $R_S$ ,  $C_S$ , and  $C_F$  versus time – red lead oxide primer + 2.6 mils topcoat.

OXIDE PRIMER  
2.6 MILS TOPCOAT

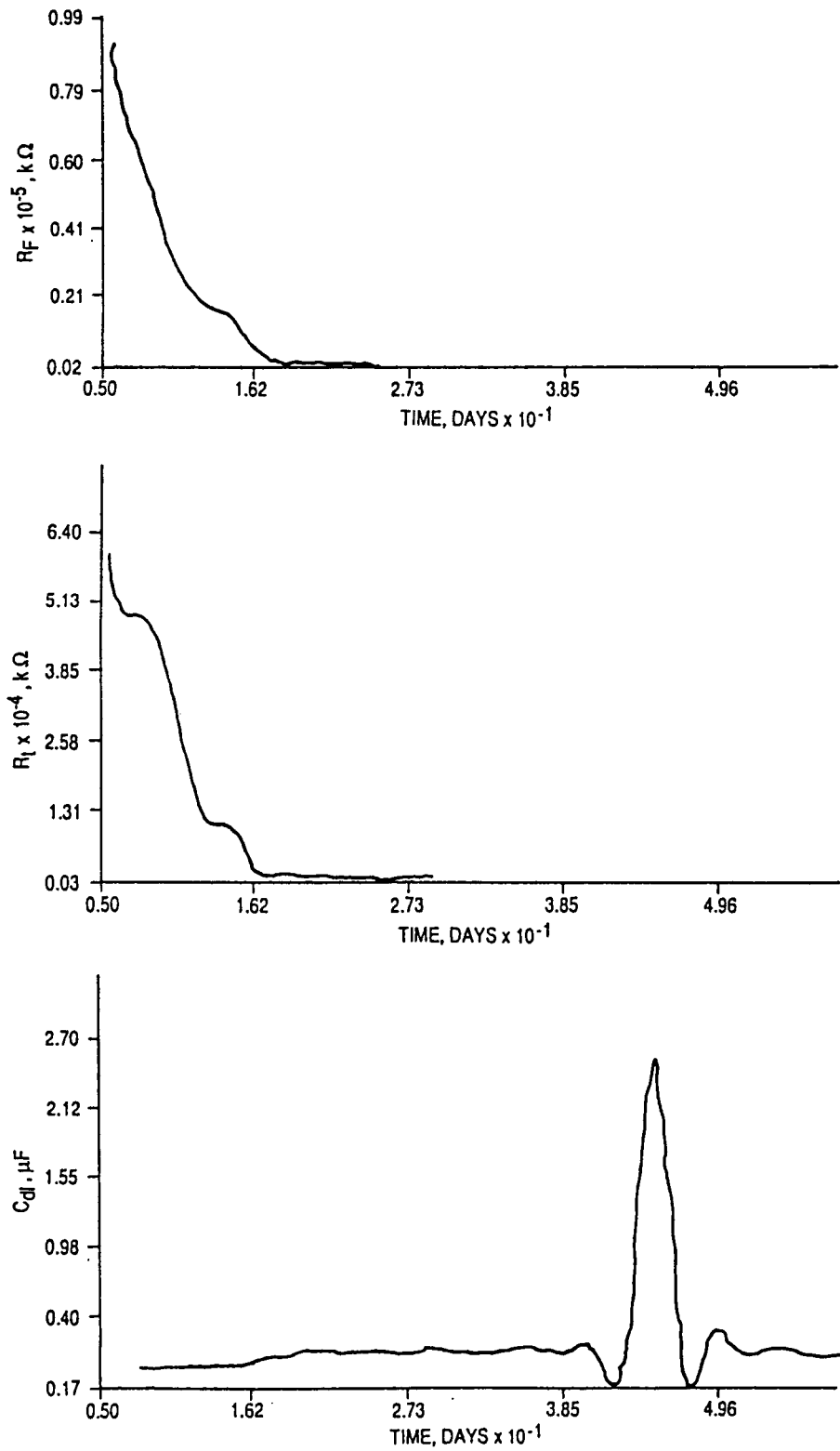


Figure 39.  $R_f$ ,  $R_t$ , and  $C_{dl}$  versus time – red lead oxide primer + 2.6 mils topcoat.

**OXIDE PRIMER  
2.6 MILS TOPCOAT**

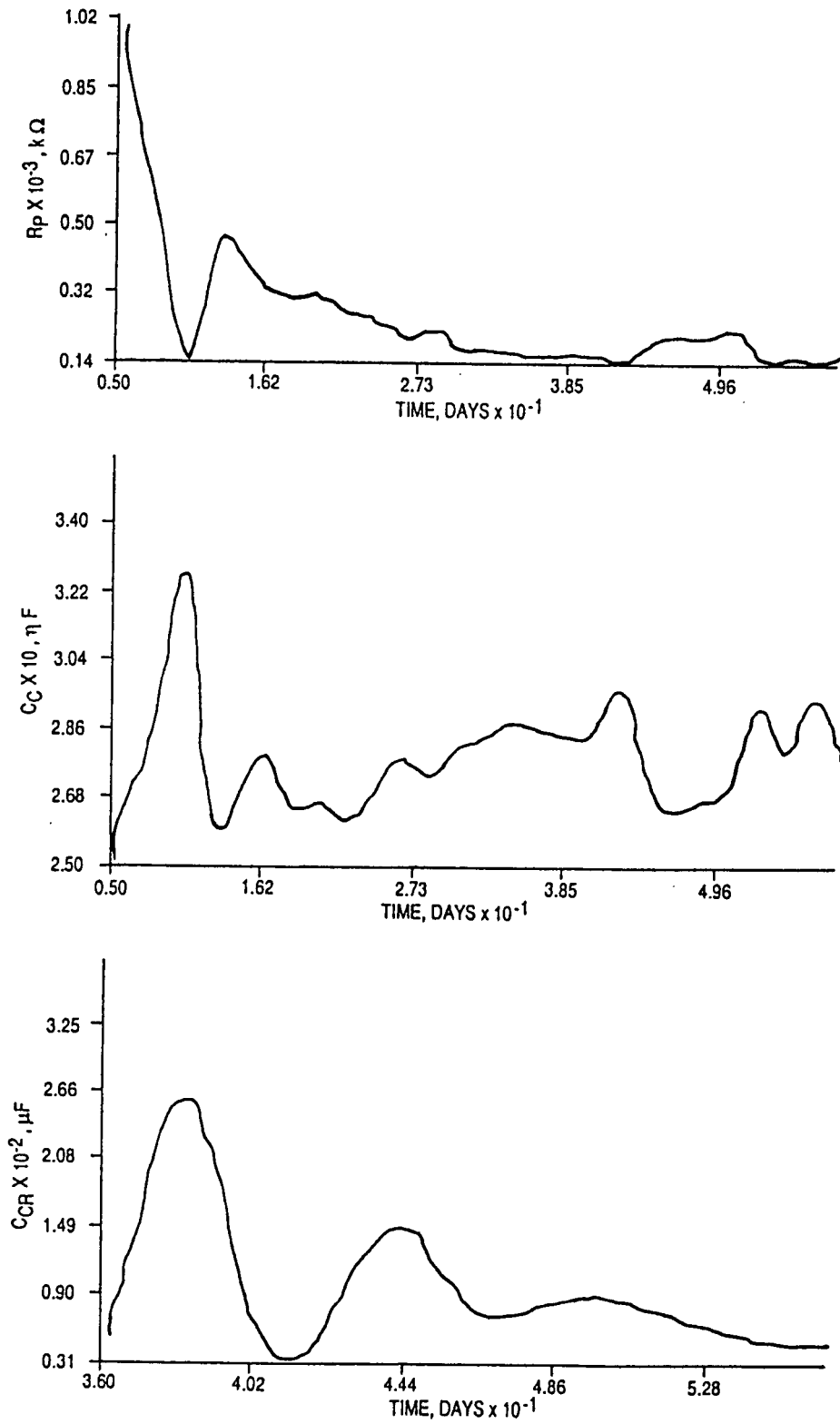


Figure 40.  $R_p$ ,  $C_c$ , and  $C_{CR}$  versus time – red lead oxide primer + 2.6 mils topcoat.

OXIDE PRIMER  
2.6 MILS TOPCOAT

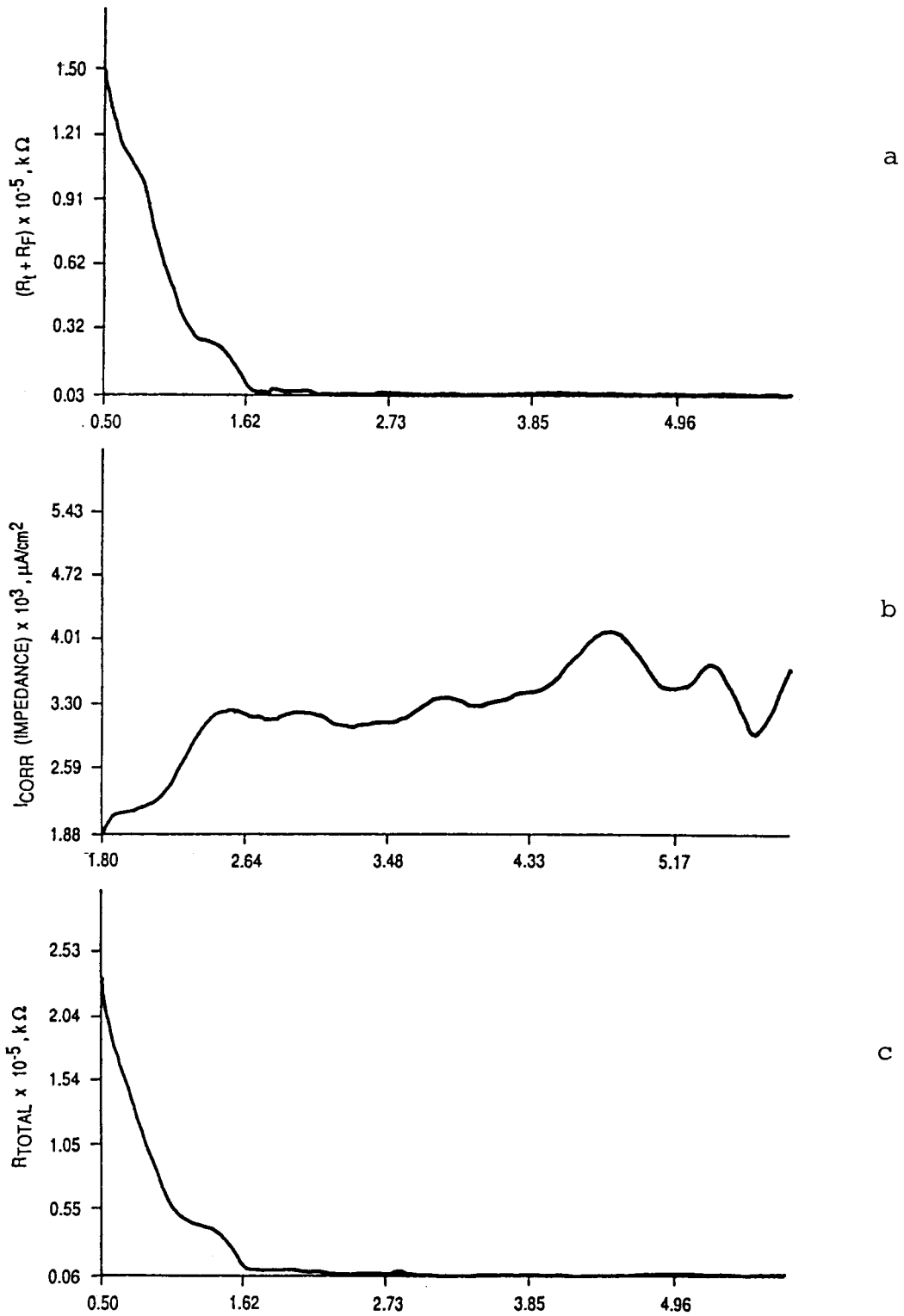


Figure 41.  $(R_t + R_f)$ ,  $I_{CORR}$  (impedance), and  $R_{total}$  versus time – red lead oxide primer + 2.6 mils topcoat.

$$\text{Corrosion rate (mpy)} = 0.1280 I_{\text{CORR}} (\text{Eq. Wt.})/\rho \quad (2)$$

where

$$I_{\text{CORR}} = \text{corrosion current density, } \mu\text{A}/\text{cm}^2$$

$$\text{Eq. Wt.} = \text{equivalent weight of corroding species, gm}$$

$$\rho = \text{density of corroding species, gm}/\text{cm}^3$$

For 4130 steel, Eq. Wt. = 27.38 gm and  $\rho = 8.0 \text{ gm}/\text{cm}^3$ , therefore

$$\text{Corrosion rate} = 0.44082 I_{\text{CORR}} \quad (3)$$

In Table 2, the average corrosion rates for each system, obtained with the DC method, are given in mils per year.

TABLE 2. AVERAGE VALUES OF CORROSION RATES FROM AC IMPEDANCE AND DC MEASUREMENTS

System	From Impedance (mpy)	DC (mpy)	$C_{\text{CR}}, \mu\text{F}$
(a) Oxide Primer	1.340	1.054	94,451
(b) Zinc-Rich Primer	0.688	0.225	31,614
(a) Oxide Primer + 0.7 mil Topcoat	0.014	0.013	—
(b) Zinc-Rich Primer + 0.7 mil Topcoat	0.205	0.194	7,345
(a) Oxide Primer + 2.6 mils Topcoat	0.00136	0.00089	93.5
(b) Zinc-Rich Primer + 2.3 mils Topcoat	0.00093	0.00220	51.3

For the AC impedance method, corrosion rates were estimated using the equation (1) with its associated assumptions for values of the Tafel slopes. For values of the polarization resistances in equation (1), it was assumed that the rate controlling resistances are the total charge transfer resistance ( $R_t + R_f$ ). Average values for corrosion rates using this technique are also listed in Table 2 and compared to the DC results.

As stated earlier, the addition of the capacitance  $C_{CR}$  to the equivalent circuit in Figure 4 not only produced a better fit to the observed Bode magnitude curve, but its value was found to be directly proportional to the corrosion current and hence the corrosion rate. Table 2 compares values of  $C_{CR}$  to the corrosion rates obtained by the AC impedance and DC polarization resistance techniques. Figure 42 is a calibration curve relating the corrosion rate to  $C_{CR}$ . Since both the zinc-rich and red lead oxide systems were used to construct this curve, it is probable that the corrosion rate of any system can be estimated using this method. Values of  $I_{CORR}$  can be obtained directly by the equation:

$$I_{CORR} = 3.4074 \times 10^{-5} C_{CR} \mu A/cm^2 \quad (4)$$

Once  $I_{CORR}$  is known, the corresponding value of the corrosion rate can be obtained with equation (2).

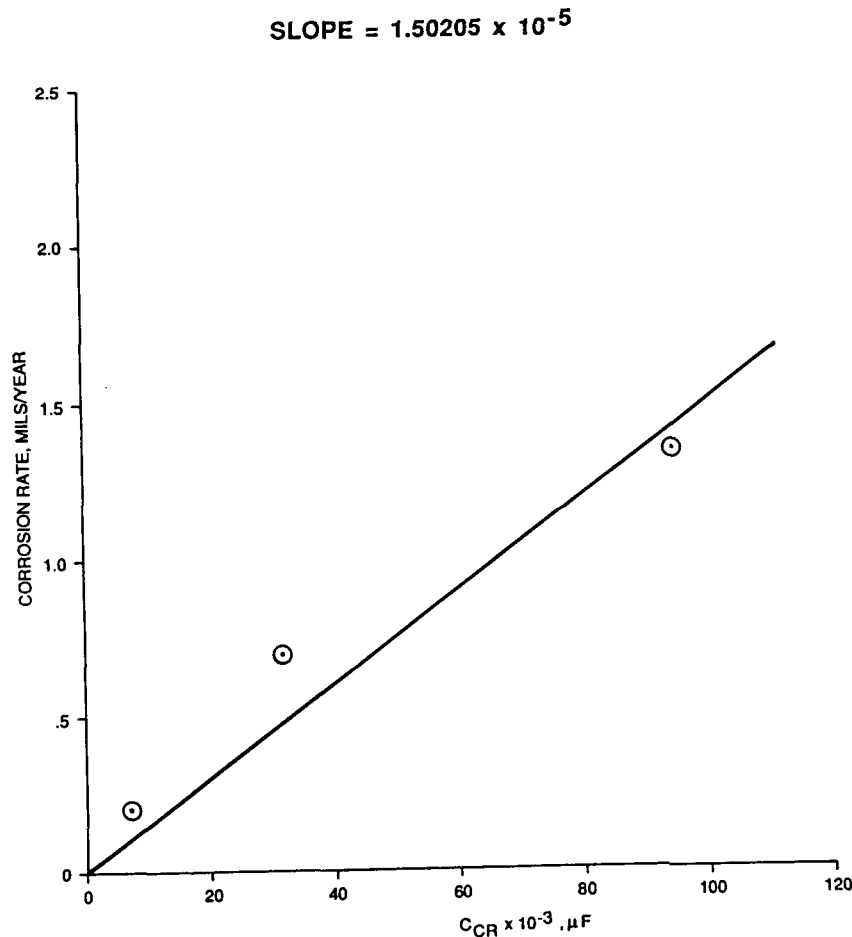


Figure 42. Calibration curve for  $C_{CR}$ .

## CONCLUSIONS

This work has demonstrated the value of the electrochemical methods in evaluating primer-topcoat systems. The AC impedance technique was effective in evaluating systems in all three phases of experimentation, which included paint systems up to 4.5 mils thick. The DC method was useful for the systems of Phase I (primer only systems) but relatively ineffective for Phase III (primer + 2 mils topcoat) systems due to the large uncertainty of this method in measuring small corrosion rates. In general, the two methods correlate very well, particularly in Phase I systems. Phase III systems showed little correlation due to the shortcomings of the DC method. The new equivalent circuit (Fig. 4) model proved effective not only in providing an exceptional fit to experimental data, but in establishing new methods of estimating corrosion rates of painted metals. The value of the extra capacitor in this circuit was determined to be directly proportional to the corrosion rate, and was calibrated using average values of  $C_{CR}$  from the systems of Phases I and II. Values for corrosion currents of the Phase III systems calculated with equation (4) agreed very well with the observed values. Thus, the corrosion rate of any metal-primer-topcoat system may be estimated by this method.

Comparison of the two primers in the primer topcoat systems resulted in contradictory conclusions. In Phase I, the zinc-rich primer gave the best protection, as seen by comparing the  $I_{CORR}$  versus time curves (Figs. 10b and 15b). In the Phase II systems, early failure in the zinc-rich system occurred, in the form of blisters on the sample surface. These blisters were caused by the hydrogen evolution reaction (product of zinc metal in the primer with hydrogen ions) occurring beneath the thin topcoat, which was inadequate in preventing penetration of the corrodent through the topcoat. The red lead oxide system, however, remained intact up to day 45, with very low corrosion rates compared to the zinc-rich system. Thus, in Phase II, the red lead oxide system provided the best protection. In Phase III, both systems provided good protection during the entire immersion time. Although loss of resistance was observed in both systems, complete coating failure did not occur in either system. The corrosion rates were comparable. Thus, in Phase III, both systems performed about equally well. This work, therefore indicates that care must be taken to use adequately thick applications of topcoat (depending on type of topcoat) over zinc-rich primer, and that the nominal coating thicknesses employed for the solid rocket boosters of the STS (Phase III tests) are shown to be satisfactory. Also, when nominal coating thicknesses are used, this work does not indicate a preference for either of the two primer-topcoat systems.

## REFERENCES

1. Mansfeld, F.: Recording and Analysis of AC Impedance Data for Corrosion Studies, Part I. Corrosion, Vol. 36, 1981, p. 301.
2. Mansfeld, F., Kending, M. W., and Tsai, S.: Recording and Analysis of AC Impedance Data for Corrosion Studies, Part II. Corrosion, Vol. 38, 1982, p. 570.
3. Danford, M. D., and Knockemus, M. W.: The Corrosion Mechanisms for Primer Coated 2219-T87 Aluminum. NASA Technical Paper 2715, April 1987.
4. Busing, W. R., and Levy, H. A.: A General Non-Linear Least Squares Program, ORGLS. Oak Ridge National Laboratory, 1958.
5. Gerchakov, S. M., Udey, L. R., and Mansfeld, F.: An Improved Method for Analysis of Polarization Resistance Data. Corrosion, Vol. 37, p. 696.
6. Danford, M. D., and Higgins, R. H.: An Electrochemical Study of the Corrosion of Primer Coated 2219-T87 Aluminum. NASA Technical Paper 2459, April 1985.
7. Stern, M., and Geary, A. L.: Journal of the Electrochemical Society, Vol. 102, 1955, p. 609.
8. Stern, M., and Geary, A. L.: Journal of the Electrochemical Society, Vol. 104, 1957, p. 56.
9. Stern, M.: Corrosion 14, 440t (1958).

1. REPORT NO. NASA TP-2820		2. GOVERNMENT ACCESSION NO.		3. RECIPIENT'S CATALOG NO.	
4. TITLE AND SUBTITLE An Electrochemical Study of Corrosion Protection by Primer-Topcoat Systems on 4130 Steel With AC Impedance and DC Methods				5. REPORT DATE May 1988	
				6. PERFORMING ORGANIZATION CODE	
7. AUTHOR(S) M. J. Mendrek, R. H. Higgins, and M. D. Danford				8. PERFORMING ORGANIZATION REPORT #	
9. PERFORMING ORGANIZATION NAME AND ADDRESS George C. Marshall Space Flight Center Marshall Space Flight Center, Alabama 35812				10. WORK UNIT NO. M-587	
				11. CONTRACT OR GRANT NO.	
12. SPONSORING AGENCY NAME AND ADDRESS National Aeronautics and Space Administration Washington, D.C. 20546				13. TYPE OF REPORT & PERIOD COVERED Technical Paper	
				14. SPONSORING AGENCY CODE	
15. SUPPLEMENTARY NOTES Prepared by Materials and Processes Laboratory, Science and Engineering Directorate.					
16. ABSTRACT <p>In an effort to investigate metal surface corrosion and the breakdown of metal protective coatings, the AC impedance method was applied to six systems of primer coated and primer topcoated 4130 steel. Two primers were used: a zinc-rich epoxy primer and a red lead oxide epoxy primer. The epoxy-polyamine topcoat was used in four of the systems. The EG&amp;G-PARC Model 368 AC impedance measurement system, along with DC measurements with the same system using the polarization resistance method, was used to monitor changing properties of coated 4130 steel disks immersed in 3.5 percent NaCl solutions buffered at pH 5.4 over periods of 40 to 60 days. The corrosion system can be represented by an electronic analog called an equivalent circuit that consists of resistors and capacitors in specific arrangements. This equivalent circuit parallels the impedance behavior of the corrosion system during a frequency scan. Values for the resistors and capacitors, that can be assigned in the equivalent circuit following a least squares analysis of the data, describe changes that occur on the corroding metal surface and in the protective coatings. Two equivalent circuits have been determined that predict the correct Bode phase and magnitude of the experimental sample at different immersion times. DC corrosion current density data are related to equivalent circuit element parameters. Methods for determining corrosion rate with AC impedance parameters are verified by the DC method.</p>					
17. KEY WORDS Electrochemical techniques Primer-topcoat systems AC impedance Polarization resistance			18. DISTRIBUTION STATEMENT Unclassified-  Subject Category: 26		
19. SECURITY CLASSIF. (of this report) Unclassified		20. SECURITY CLASSIF. (of this page) Unclassified		21. NO. OF PAGES 55	22. PRICE